Circulation

ORIGINAL RESEARCH ARTICLE

Pkm2 Regulates Cardiomyocyte Cell Cycle and Promotes Cardiac Regeneration

BACKGROUND: The adult mammalian heart has limited regenerative capacity, mostly attributable to postnatal cardiomyocyte cell cycle arrest. In the last 2 decades, numerous studies have explored cardiomyocyte cell cycle regulatory mechanisms to enhance myocardial regeneration after myocardial infarction. Pkm2 (Pyruvate kinase muscle isoenzyme 2) is an isoenzyme of the glycolytic enzyme pyruvate kinase. The role of Pkm2 in cardiomyocyte proliferation, heart development, and cardiac regeneration is unknown.

METHODS: We investigated the effect of Pkm2 in cardiomyocytes through models of loss (cardiomyocyte-specific Pkm2 deletion during cardiac development) or gain using cardiomyocyte-specific Pkm2 modified mRNA to evaluate Pkm2 function and regenerative affects after acute or chronic myocardial infarction in mice.

RESULTS: Here, we identify Pkm2 as an important regulator of the cardiomyocyte cell cycle. We show that Pkm2 is expressed in cardiomyocytes during development and immediately after birth but not during adulthood. Loss of function studies show that cardiomyocyte-specific Pkm2 deletion during cardiac development resulted in significantly reduced cardiomyocyte cell cycle, cardiomyocyte numbers, and myocardial size. In addition, using cardiomyocyte-specific Pkm2 modified RNA, our novel cardiomyocyte-targeted strategy, after acute or chronic myocardial infarction, resulted in increased cardiomyocyte cell division, enhanced cardiac function, and improved long-term survival. We mechanistically show that Pkm2 regulates the cardiomyocyte cell cycle and reduces oxidative stress damage through anabolic pathways and β-catenin.

CONCLUSIONS: We demonstrate that Pkm2 is an important intrinsic regulator of the cardiomyocyte cell cycle and oxidative stress, and highlight its therapeutic potential using cardiomyocyte-specific Pkm2 modified RNA as a gene delivery platform.

Ajit Magadum, PhD
Neha Singh, PhD
Ann Anu Kurian, BS
Irsa Munir, MD
Talha Mehmood, MD
Kemar Brown, MD
Mohammad Tofael Kabir Sharkar, PhD
Elena Chepurko, DVM
Yassine Sassi, PhD
Jae Gyun Oh, PhD
Philyoung Lee, PhD
Celio X.C. Santos, PhD
Avital Gaziel-Sovran, PhD
Guoan Zhang, PhD
Chen-Leng Cai, PhD
Changwon Kho, PhD
Manuel Mayr, MD, PhD
Ajay M. Shah, MD
Roger J. Hajjar, MD
Lior Zangi, PhD

Key Words: anabolism ■ cardiomyocytes ■ cell proliferation ■ regeneration

Sources of Funding, see page 1264

https://www.ahajournals.org/journal/circ

Clinical Perspective

What Is New?

- We developed novel therapeutic cardiomyocyte-specific modified RNA that allows transient expression of any gene of interest exclusively in cardiomyocytes.
- We established that Pkm2 (pyruvate kinase muscle isoenzyme 2) expression is downregulated during mammalian heart development, which coincides with the mammalian heart regeneration window.
- We identified Pkm2 as a previously unknown inducer of cardiomyocyte proliferation in vitro and in vivo.
- We demonstrated that Pkm2 interacts with β-catenin and activates both G6pd and the pentose phosphate pathway to provide nucleotides for DNA synthesis and reduce oxidative stress after myocardial infarction.
- We showed that cardiomyocyte-specific Pkm2 modified RNA expression induces cardiac regeneration after myocardial infarction.

What Are the Clinical Implications?

- The cardiomyocyte-specific modified RNA expression platform can be used for gene delivery in clinical applications to treat heart diseases.
- The identification of Pkm2, a previously unrecognized inducer of cardiomyocyte proliferation and inhibitor of oxidative stress in the heart after myocardial infarction, shows the gene regulates multiple processes and has a pleiotropic beneficial effect on the heart after myocardial infarction.
- Our cardiomyocyte-specific modified RNA expression platform will enable the development of a new class of therapeutics for different diseases beyond cardiology. The gene can be delivered therapeutically to specific cells or organs undergoing disease states.

The mammalian heart has a short window of regenerative capacity immediately after birth via cardiomyocyte cell division;[1] however, this capacity is lost 1 week after birth.[1] Recent studies showed that Hippo[2–5] or NRG1-ERBB2-ERBB4[6,7] pathways activate β-catenin, which induces cardiomyocyte cell division. In parallel, other recent work demonstrated that increased oxidative stress in the early postnatal window is associated with a shift from glycolytic to oxidative metabolism and plays pivotal roles in cardiomyocyte cell cycle arrest. Importantly, inhibition of oxidative stress in postnatal cardiomyocytes leads to reduced oxidative DNA damage and curtailed cell cycle arrest.[8–10] To date, however, it is unclear whether these seemingly unrelated nodal cardiomyocyte cell division pathways are interlinked. Therefore, we set out to identify an upstream regulator of both β-catenin and oxidative stress pathways in cardiomyocytes. We hypothesized that glycolytic enzymes involved in regulating oxidative stress and β-catenin may act as nodal regulators of the cardiomyocyte cell cycle. Of these 18 glycolytic enzymes, only 1 is known to interact with β-catenin. The dimer form of the glycolytic enzyme Pkm2 (pyruvate kinase muscle isoenzyme 2) has been extensively studied in cancer cells.[11–15] We know dimer Pkm2 directly interacts with β-catenin in prostate cancer cells[13] and promotes metabolic flux into the pentose phosphate pathway (PPP), activation of which results in less oxidative DNA damage in a cervical cancer cell line.[15] Accordingly, we hypothesized that Pkm2 may play a central role in cardiomyocyte cell division during development and immediately after birth and could also be a therapeutically effective target to enhance myocardial regeneration. Pkm2 and its alternatively splicing mRNA Pkm1 are both produced by the *PKM* gene.[11,16] Pkm2 and Pkm1 modulate the conversion of PEP (phosphoenolpyruvate) and ADP (adenosine diphosphate) to pyruvate and ATP (adenosine triphosphate).[17–20] Pkm1 is active and expressed in adult tissues, like muscle and brain, that consistently need high levels of energy,[21,22] whereas Pkm2 is expressed in most cell types at varying levels.[19,23] Pkm2, which is enzymatically slower than Pkm1, reduces pyruvate kinase activity and promotes the alternate anabolic glycolytic pathway, the PPP, which prevents oxidative stress.[14,24–26] To date, Pkm2 studies in cardiac development during adulthood and after injury are limited, but suggest that Pkm2 may be induced in adult cardiomyocytes under stress conditions.[27–30] The role of Pkm2 in cardiomyocyte cell cycle regulation remains unknown.

In this article, we examine the role of Pkm2 in cardiomyocytes during normal embryonic and postnatal development as well as after injury. Using gain and loss of function models, we demonstrate that Pkm2 activates 2 separate and synergistic enzymatic and nonenzymatic pathways in cardiomyocytes to induce the cardiomyocyte cell cycle and cardiac regeneration post injury.

METHODS

The data, analytic methods, and study materials will be been made available to other researchers for purposes of reproducing the results or replicating the procedure that has been presented in this article.

Mice

All animal procedures were performed under protocols approved by the Institutional Animal Care and Use Committee at the Icahn School of Medicine at Mount Sinai. CFW or Rosa26^{mTmG} mice strains, male and female, were used. Different modified RNAs (modRNAs; 100 or 150 μg/heart) were injected directly into the myocardium during open chest surgery. Three to 8 animals were used for each experiment. For long-term survival, 8- to 10-week-old CFW mice, treated with cardiomyocyte-specific modRNAs (n=10) after

myocardial infarction (MI) induction, were allowed to recover for 6 months in the animal facility. Deaths were monitored and documented. Tamoxifen-inducible cardiomyocyte-restricted deletion of Pkm2 ($_{CMS}$KO-Pkm2) was generated by crossing Pkm2$^{flox/flox}$ (purchased from Jackson Laboratories [B6;129S-Pkmtm1.1Mgvh/J]) to Tnnt2$^{MerCreMer/+}$ mice (made by Dr Chen-Leng Cai, a coauthor on this article). Tamoxifen (Sigma-Aldrich) was dissolved in sesame oil at 10 mg/ml as stock solution. To induce Cre nuclear translocation, tamoxifen was administered to mice by intraperitoneal injection for 2 consecutive days (E9-E10; 24-hour interval between administrations) at 0.05 mg/g body weight/day for embryonic stages. The tissues were harvested on E18 for analysis. Mouse husbandry was carried out according to the protocol approved by the Institutional Animal Care and Use Committee at Icahn School of Medicine at Mount Sinai. Oligonucleotide sequences for genotyping these mouse lines: Tnnt2-F-AGGAACATGAAATCCAGGGTGGCT, Tnnt2-R- GTTCAGCATCCAACAAGGCACTGA; and Pkm2-F-CCTTCAGGAAGAC- AGCCAAG, Pkm2-R – AGTGCTGCC TGGAATCCTCT.

modRNA Synthesis

modRNAs were transcribed in vitro from plasmid templates (see complete list of open reading frame sequences used to make modRNA in Table I in the Data Supplement). Using a customized ribonucleotide blend of antireverse cap analog, 3´-O-Me-m7G(5′)ppp(5′)G (6 mmol/L, TriLink Biotechnologies), GTP (guanosine triphosphate; 1.5 mmol/L, Life Technology), ATP (7.5 mmol/L, Life Technology), CTP (cytidine triphosphate; 7.5 mmol/L, Life Technology), and N1-Methylpseudouridine-5′-Triphosphate (7.5 mmol/L, TriLink Biotechnologies), as described previously in our recent protocol paper,[31] mRNA was purified using the Megaclear kit (Life Technology) and treated with antarctic phosphatase (New England Biolabs), followed by repurification using the Megaclear kit. mRNA was quantitated by Nanodrop (Thermo Scientific), precipitated with ethanol and ammonium acetate, and resuspended in 10 mmol/L TrisHCl, 1 mmol/L EDTA.

modRNA Transfection

In vivo modRNA transfection was done, as described previously in our recent method paper,[32] using sucrose citrate buffer containing 20 µl of sucrose in nuclease-free water (0.3 g/ml) and 20 µl of citrate (0.1 mol/L pH=7; Sigma) mixed with 20 µl of different modRNA concentrations in saline to a total volume of 60 µl. The transfection mixture was directly injected (3 individual injections, 20 µl each) into the myocardium. For in vitro transfection, we used RNAiMAX transfection reagent (Life Technologies) according to manufacturer's recommendations.

Statistical Analysis

Statistical significance was determined by unpaired 2-tailed *t* test, 1-way ANOVA, Tukey multiple comparison test, and Bonferroni post hoc test or log-rank (Mantel-Cox) test for survival curves, as detailed in respective figure legends. *P* value <0.05 was considered significant. All graphs represent average values, and values were reported as mean±SEM. Unpaired 2-tailed *t* test was based on assumed normal distributions. To quantify the number of CD31 luminal structures, we used wheat agglutinin, OHG, CD45, CD3, positive TUNEL, BrdU, ki67, pH3, or Aurora B cardiomyocytes, with results acquired from at least 3 heart sections/heart, in numbers of mice as mentioned in respective figure legends.

Detailed methods are available in the Data Supplement.

RESULTS

First, we evaluated Pkm splice variants (Pkm2 and Pkm1) for their expression during cardiac development, adulthood and after injury (Figure 1, Figures I and II in the Data Supplement). Figure I in the Data Supplement shows that embryonic hearts uniquely express both Pkm2 and Pkm1 in high amounts, as compared with embryonic kidneys or lungs, organs known to express high levels of Pkm2.[20,27] Both cardiomyocytes and noncardiomyocytes express Pkm2 (Figure 1C, please see complete list of antibodies used in this study in Table II in the Data Supplement), though its expression levels significantly decline in P7 (Figure 1A through 1F). In adulthood, however, Pkm2 expression in adult cardiomyocytes is very low (Figure 1). We demonstrate, in agreement with previous studies,[28,30] that after ischemic injury (eg, MI), Pkm2 expression rises moderately in cardiomyocytes (1.8-fold increase, $P \leq 0.05$) and significantly in noncardiomyocytes, including leucocytes (7-fold, $P \leq 0.001$; Figure 1G and 1H and Figure IIc in the Data Supplement; please see complete list of primer sequences for quantitative polymerase chain reaction used in this study in Table III in the Data Supplement).

Next, we wanted to determine if restoring Pkm2 levels in postnatal cardiomyocytes can induce their cell cycle in vitro and after MI. For Pkm2 upregulation in cardiomyocytes, we used our previously described modRNA technology that enables highly efficient, transient, local, nonimmunogenic gene delivery to cardiac cells, including cardiomyocytes, in vitro and in vivo.[31–34] We used luciferase modRNA as a control gene for Pkm2 modRNA because they are similarly sized (~1.6Kb) and luciferase has no biological function in mice. Pkm2 delivery with modRNA technology might also boost Pkm2 expression in noncardiomyocytes, thereby increasing their cellular division and possibly promoting undesired effects, such as elevation in fibrosis and immune response, or preventing cardiomyocyte cell division after MI.[35] To avoid these effects, and to test Pkm2's ability to boost cardiomyocytes' cell cycle and cardiac regenerative capacity, we developed a unique circuit modRNA, which leads to cardiomyocyte-specific modRNA ($_{cms}$modRNA) delivery. This system is based on 2 distinct modRNA constructs (Figure 2A and 2B; Figures III and IV in the Data Supplement). The first contains L7Ae, an archaeal ribosomal protein that regulates the translation of genes containing a kink-turn motif, a specific binding site for L7Ae.[36,37] L7Ae protein suppresses translation of

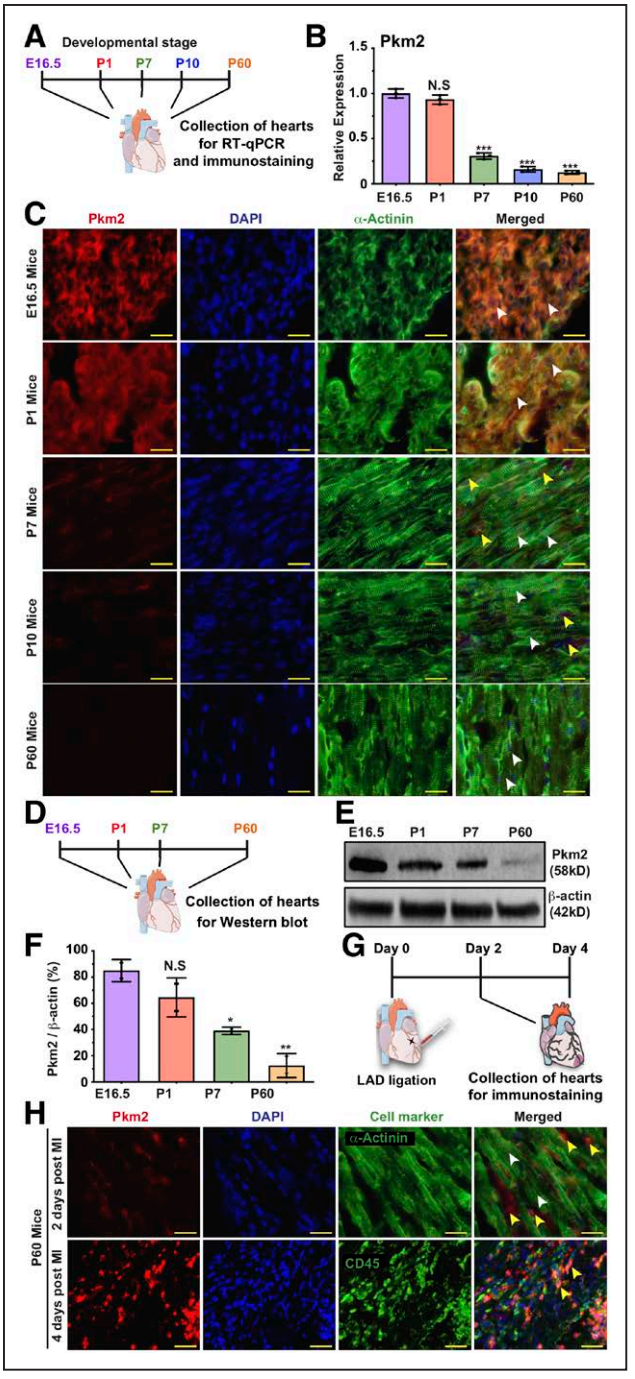

Figure 1. Pkm2 expression in cardiomyocytes during different stages of heart development and after myocardial infarction.
A, Experimental timeline for Pkm2 quantitative real-time polymerase chain reaction (qRT-PCR) and immunostaining with Pkm2 and α-Actinin (cardiomyocyte marker) at different stages of mouse heart development. **B**, Relative expression of Pkm2 measured by qRT- PCR in mice hearts (E16.5, P1, P7, P10 or P60), n=3. **C**, Representative images of Pkm2 expression at different stages of mouse heart development. **D**, Experimental plan for Pkm2 Western blot analysis at different stages of mouse heart development. **E**, Western blot Pkm2. **F**, Quantitative analysis of **E**, n=2. **G**, Experimental plan for immunostaining Pkm2 and α-Actinin or CD45 (leukocyte marker) at different time points after myocardial infarction (MI). **H**, Representative images of Pkm2 expression at different time points after MI. White arrowheads point to cardiomyocytes. Yellow arrowheads point to noncardiomyocytes. One-way ANOVA, Tukey's multiple comparison test for **B** and **F**. ***P<0.001, **P<0.01, *P<0.05, N.S, not significant. Scale bar, 25 μm. DAPI indicates 4′,6-diamidino-2-phenylindole; LAD, left anterior descending coronary artery; and Pkm2, pyruvate kinase muscle isoenzyme 2.

the designed modRNA gene of interest by binding to the kink-turn motif upstream of the modRNA sequence when the 2 constructs are cotransfected into the cell. We achieved cardiomyocyte specificity by adding a cardiomyocyte-specific microRNA recognition element to the 3'UTR of the L7Ae gene. We prevented L7Ae translation in cardiomyocytes that abundantly and mostly exclusively express those miRs, thereby allowing the gene of interest modRNA to translate strictly in cardiomyocytes (Figure 2A and 2B; Figures III and IV in the Data Supplement).

Because a number of groups have shown that miR1-1[38] and miR-208a[39] are expressed exclusively in cardiomyocytes, we designed an L7Ae modRNA called miR-1-208 that contains both miR1-1 and miR-208a recognition elements and used Pkm2 (Pkm2-K), nuclear green fluorescent protein (GFP), and Cre recombinase modRNAs that contain a kink-turn motif. In neonatal cardiomyocytes in vitro, and our mouse MI model in vivo, transfecting Pkm2-K or nuclear GFP modRNA resulted in translating the gene of interest in both cardiomyocytes and noncardiomyocytes. However, during cotransfection with miR-1-208, the gene of interest was exclusively translated in cardiomyocytes, in other words, not in noncardiomyocytes (eg, endothelial or smooth muscle cells; Figure 2B; Figure V in the Data Supplement). In vivo, intramyocardial delivery of Cre K modRNA in our MI model, using Rosa26 reporter mice (Rosa26^{mTmG}), resulted in GFP expression in cardiomyocytes and noncardiomyocytes covering ≈50% of the left ventricle (LV). However, cotransfecting Cre recombinase modRNA with miR-1-208 ($_{CMS}$Cre) labeled only cardiomyocytes covering ≈20% of the LV (Figure 2B through 2D; Figure IVa and IVb in the Data Supplement). In addition, no Cre-Lox recombination could be seen in the spleen, lung or liver after intramyocardial delivery of $_{CMS}$Cre modRNA (Figure IVc in the Data Supplement). As L7Ae is a foreign protein in mice, we thought it might induce an immune response. We therefore evaluated CD45, CD3, or TUNEL expression 7 days after MI in hearts injected with modRNA with or without L7Ae. Our data indicate that L7Ae did not elevate immune cell infiltration or cell death after MI (Figure VI in the Data Supplement). We hypothesize that because the heart already contains high levels of inflammation and cell death after MI, adding L7Ae did not change these processes.

We initially tested Pkm2 modRNA kinetics and its capacity to increase cell cycle markers in cardiomyocytes in vitro. We show that Pkm2 modRNA increased protein expression for at least 8 days, and elevated cardiomyocyte cell cycle marker expression and overall numbers in Pkm2-transfected neonatal rats, in comparison with luciferase modRNA controls, 3 or 7 days after transfection, respectively (Figure VII in the Data Supplement). In vivo, directly injecting Pkm2 modRNA into

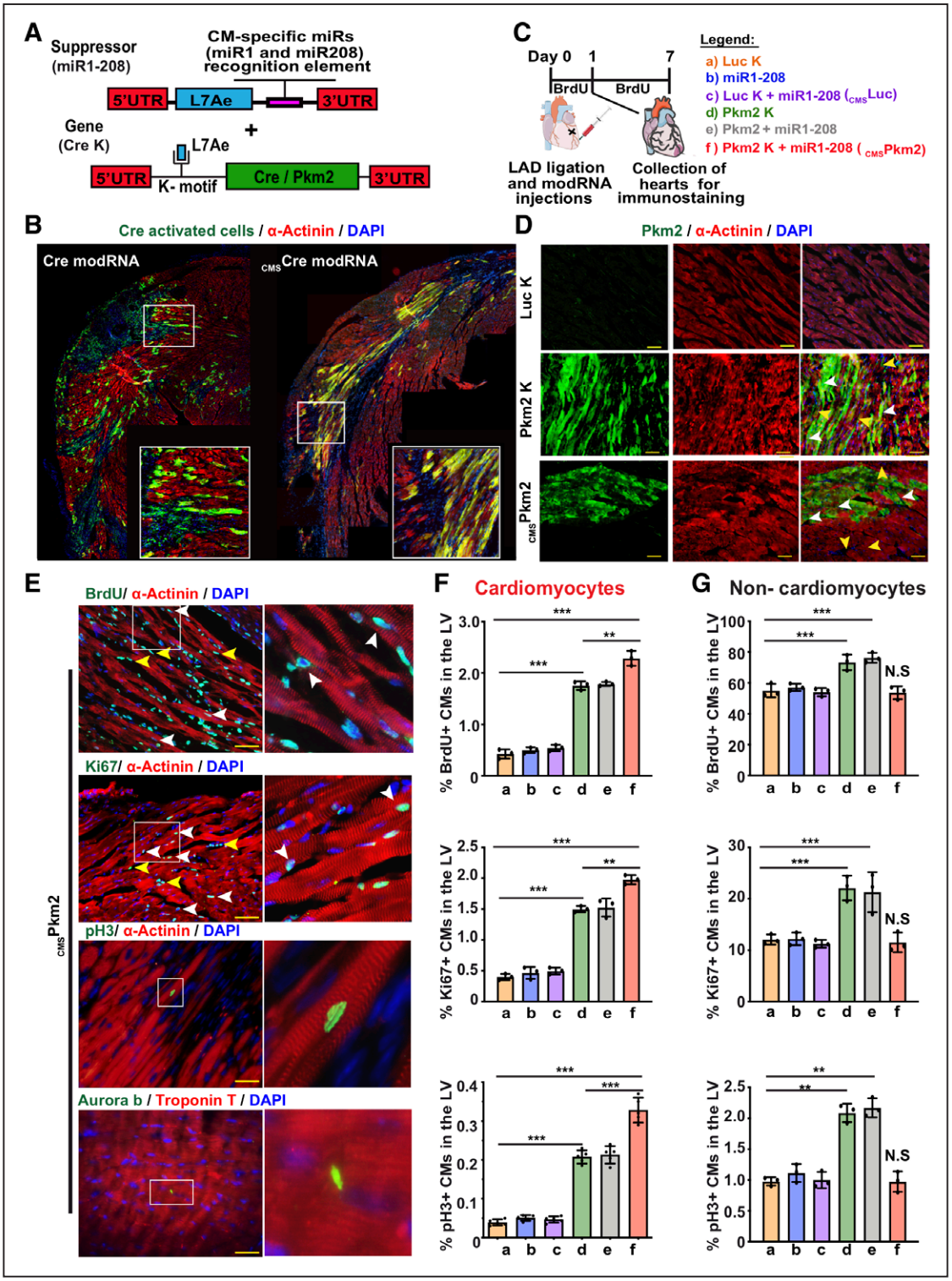

Figure 2. Transient and exclusive Pkm2 in cardiomyocytes, delivered using cardiomyocyte-specific Pkm2 modified RNA, increases cell cycle markers in postnatal cardiomyocytes.

A, Experimental design to evaluate the cardiomyocyte-specific (CMS) modified RNA (modRNA) expression tool using Rosa26mTmG mice, which were transfected with either Cre modRNA alone or CMSCre modRNA immediately after myocardial infarction (MI). Seven days later, hearts were collected and stained for green fluorescent protein (GFP), α-Actinin and DAPI. **B**, Representative images of Rosa26mTmG adult mouse heart 7 days after myocardial infarction (MI) and delivery of either Cre modRNA alone or CMSCre modRNA. **C**, Experimental timeline for evaluating cmsPkm2 modRNA expression (day 1) and effect (day 7) on cell cycle markers (Brdu, Ki67 and pH3) in cardiomyocytes and noncardiomyocytes. **D**, Representative images of Pkm2 expression in cardiomyocytes and noncardiomyocytes 1 day after MI and delivery of luciferase (Luc) K, Pkm2 K, or CMSPkm2 modRNA. **E**, Representative images of cycle markers (BrdU, Ki67, pH3, and Aurora B) expression in cardiomyocytes 7 days after MI and delivery of CMSPkm2 modRNA. **F** and **G**, Quantification of cell cycle markers in cardiomyocytes (**F**) or noncardiomyocytes (**G**) 7 days after MI (n=3). One-way ANOVA, Tukey's Multiple Comparison Test for **F** and **G**. ***P<0.001, **P<0.01. N.S, not significant. Scale bar, 50 μm (**D**) and 25 μm (**E**). CM indicates cardiomyocyte; DAPI, 4′,6-diamidino-2-phenylindole; LAD, left anterior descending coronary artery; and Pkm2, pyruvate kinase muscle isoenzyme 2.

the myocardium raised Pkm2 levels in cardiomyocytes and other cardiac cells (Figure VIII in the Data Supplement). Pkm2 pharmacokinetics in vivo lasted 8 to 12 days (Figure IX in the Data Supplement) with markedly more Pkm2 protein in the LV 2 days after Pkm2 modRNA delivery (Figure VIIId in the Data Supplement). To test Pkm2 modRNA's effects on the cell cycle in the context of MI, we intramyocardially delivered Luc-K, miR1-208, or Luc-K+miR1-208 ($_{CMS}$Luc), and Pkm2-K, Pkm2+miR1-208, or Pkm2-K+miR1-208 ($_{CMS}$Pkm2). Seven days after transfection we measured cell cycle markers in cardiomyocytes and noncardiomyocytes in the LV (Figure 2C). Pkm2-K or Pkm2+miR1-208 modRNA increased cell cycle markers in both cardiomyocytes and noncardiomyocytes more than luciferase modRNA (P<0.001, Figure 2E and 2F). However, $_{CMS}$Pkm2 modRNA only induced ki67- or pH3-positive cardiomyocytes (P<0.001), with no significant effect on noncardiomyocyte cell cycle markers. Live imaging of neonatal cardiomyocytes showed cardiomyocyte cell division after cotransfection with $_{CMS}$Pkm2 modRNA and $_{CMS}$nGFP modRNA but not $_{CMS}$Luc modRNA or nuclear GFP modRNA (Movie I in the Data Supplement). Further, Pkm2's effect on cell cycle markers was very prominent in the injected area after MI but subtler in both the injected areas of noninfarcted hearts and remote, uninjured areas (Figure IX in the Data Supplement).

To evaluate whether Pkm2's enhancing effects on cell cycle marker expression can lead to successful cardiomyocyte cell division after MI, we used a lineage-tracing model that combines $_{CMS}$modRNAs and a Rosa26^{mTmG} mouse model, mixing $_{CMS}$Pkm2 or $_{CMS}$Luc with $_{CMS}$Cre modRNA to generate permanently GFP-labeled cardiomyocytes (Figure 3A through 3J). We traced the fate and properties of transfected cardiomyocytes and their progeny over time (including after either $_{CMS}$Pkm2 or $_{CMS}$Luc modRNAs were no longer expressed). The number of labeled cardiomyocytes with $_{CMS}$Pkm2 + $_{CMS}$Cre modRNAs was significantly higher than control $_{CMS}$Luc + $_{CMS}$Cre modRNAs 3 and 28 days after MI (Figure 3D). This suggests that $_{CMS}$Pkm2 modRNA induces cell division in preexisting cardiomyocytes and mimics the intrinsic regeneration process observed in mice 1 day after birth.[1] Twenty-eight days after $_{CMS}$Pkm2 + $_{CMS}$Cre modRNAs treatment, GFP$^+$ cardiomyocytes showed elevated expression of cell cycle markers such as pH3 and Ki67 (Figure 3E through 3G), long after Pkm2 was no longer expressed. Heart weight to body weight ratio was significantly increased (Figure 3H), whereas both GFP$^+$ cardiomyocytes size (Figure 3I) and nuclei numbers/cell (Figure 3J) were smaller in mice treated with $_{CMS}$Pkm2 + $_{CMS}$Cre modRNAs compared with control.

Because higher cardiomyocyte numbers can be a result of improved cardiomyocyte survival, and to rigorously assess cardiomyocyte division in vivo, we used a second lineage-tracing model based on Cre-recombinase-dependent mosaic analysis with double markers (MADM) mice. As previously shown,[40,41] this system validates successful cardiomyocyte cell division by evaluating single-color cardiomyocytes among total labeled cardiomyocytes. Similar to our strategy in the Rosa26^{mTmG} lineage-tracing model, either $_{CMS}$Pkm2 or $_{CMS}$Luc modRNAs were intramyocardially delivered into heterozygous MADM-ML-11$^{GT/TG}$ mice. Fourteen days after MI and modRNA delivery, we collected hearts and determined the single-color percentage of total labeled cardiomyocytes. $_{CMS}$Pkm2 + $_{CMS}$Cre modRNAs significantly increased (P≤0.0001) the single-color percentage of total labeled cardiomyocytes, mostly in the border zone and infarct, 14 days after MI in comparison with control $_{CMS}$Luc + $_{CMS}$Cre modRNAs (Figure 3K through 3R). In addition, 14 days after MI and $_{CMS}$Pkm2 + $_{CMS}$Cre modRNA delivery, isolated adult cardiomyocytes show notably higher (P≤0.001) single-color percentage of total labeled cardiomyocytes, mostly mononuclear, in comparison with control (Figure 3M and 3P). We also used our cardiac MADM model in chronic MI, injecting modRNA 15 days after MI. Our results (Figure X in the Data Supplement) indicate, similar to the acute MI data, that $_{CMS}$Pkm2 + $_{CMS}$Cre modRNA markedly raises (P≤0.001) the single-color percentage of total labeled cardiomyocytes in the heart, in comparison with control. Thus, using 2 independent cardiomyocyte cell division lineage-tracing models, we conclusively show that Pkm2 activates cardiomyocyte cell division in vivo. Note that our $_{CMS}$modRNA platform allowed us to employ 2 separate cardiomyocyte cell division lineage-tracing models without needing to cross with cardiomyocyte-specific Cre-expressing mice, so that our approach facilitates faster and less expansive analysis of cardiomyocyte cell division in vivo.

Based on its expression during development but not after birth, ability to induce postnatal cardiomyocyte cell division after MI, and known role controlling both β-catenin and anabolic pathways in cancer cells, we wanted to investigate Pkm2's ability to increase β-catenin and anabolic pathway activity in postnatal cardiomyocytes after MI. More specifically, we evaluated the gene expression of Pkm2 transfected postnatal cardiomyocytes after MI. Because adult cardiomyocytes are challenging to sort using fluorescence activated cell sorting, owing to cardiomyocyte size and rapid cell death after isolation, we used magnetic beads to sort transfected adult cardiomyocytes. For this process, we designed a cardiomyocyte-specific inactive human CD25 modRNA based on truncated human CD25 (the only extracellular domain of the human IL2 receptor) that can be expressed on the surface of transfected adult cardiomyocytes without compromising their cell activity (owing to lack of intracellular domain), thereby allowing us to distinguish them from nontransfected cardiomyocytes. In this way, we were able to use anti-hCD25 magnetic

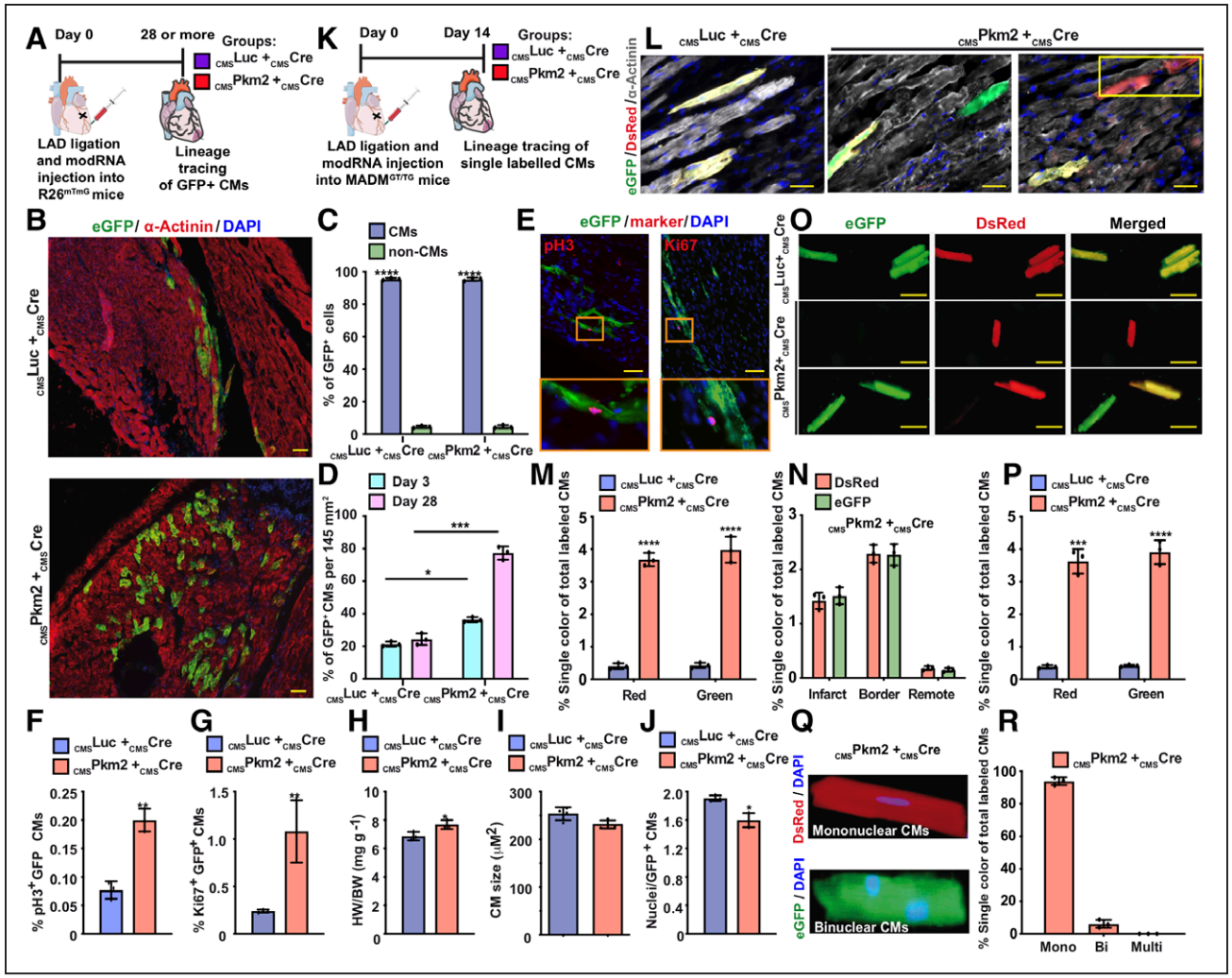

Figure 3. Lineage tracing models show that transient Pkm2 expression increase cardiomyocyte cell division and suppress postnatal cardiomyocyte cell cycle arrest.

A, Experimental timeline used for cardiac lineage tracing in R26mTmG mice. **B**, Representative images of transfected cardiomyocytes and their progeny (green fluorescent protein positive [GFP+], α-Actinin+) 28 days after MI. **C**, Quantification of GFP+ cardiomyocytes 3 or 28 days after MI, n=3. **D**, Transfection efficiency (%GFP+) of cardiomyocytes or noncardiomyocytes 28 days after myocardial infarction (MI), n=3. **E**, Representative images of GFP+ cardiomyocytes, pH3+, or Ki67+ 28 days after MI. **F** and **G**, Quantification of GFP+ pH3+, n=3 (**F**), or GFP+ Ki67+ cardiomyocytes, n=3 (**G**), 28 days after transfection with cardiomyocyte-specific Luciferase (CMSLuc) or CMSPkm2 with CMSCre modified RNA (modRNA) in MI model. **H** through **J**, Ratio of heart (HW) to body weight (BW), n=3 (**H**); relative cross-sectional area of GFP+ cardiomyocytes, n=3 (**I**); and number of nuclei in GFP+ cardiomyocytes, n=3 (**J**); in hearts 28 days after MI and delivery of CMSPkm2 in cardiac lineage tracing model using R26mTmG mice. **K**, Experimental timeline to trace proliferating cardiomyocytes using mosaic analysis with double markers (MADM) mice **L**, Representative images of single-color-labeled (Green (eGFP+/DsRed-), Red (eGFP-/DsRed+)) or double-color-labeled (Yellow (eGFP+/DsRed+) cardiomyocytes 14 days after MI and injection of CMSLuc or cmsPkm2 with CMSCre modRNA in a MADM MI mouse model. **M**, Quantification of single-color cardiomyocytes (Red or Green) amongst total labeled cardiomyocytes 14 days after MI, n=5. **N**, Distribution of single-color cardiomyocytes in the heart 14 days after MI, n=3 (infarct, border, or remote area). **O**, Representative images of isolated cardiomyocytes from MADM mice 14 days after MI and modRNA injection. **P**, Quantification of isolated single-color cardiomyocytes 14 days after MI, n=3. **Q** and **R**, Representative (**Q**) image and (**R**) quantification (mono, bi, or multi) of single-color cardiomyocyte nucleation 14 days after MI, n=3. Unpaired 2-tailed *t* test or 2-way ANOVA to analyze the data in **C** and **D**. ****P<0.0001, ***P<0.001, **P<0.01, *P<0.05, N.S, not significant. Scale bar, 50 μm (**B**) and (**L**), or 5 μm (**E**) and **O**). DAPI indicates 4′,6-diamidino-2-phenylindole; LAD, left anterior descending coronary artery; and Pkm2, pyruvate kinase muscle isoenzyme 2.

beads, which are not cross-reactive with mouse CD25, to sort transfected adult cardiomyocytes (Figure XI in the Data Supplement) and evaluate their gene expression using quantitative real time–polymerase chain reaction. Two days after MI and intramyocardial delivery of either $_{CMS}$Pkm2 or $_{CMS}$Luc together with cardiomyocyte-specific inactive human CD25 modRNAs, we measured changes in gene expression. Our results showed that isolated cells were enriched for cardiomyocyte markers with significantly lower Troponin T expression but showed little to no change in Myh6 expression, cardiac gap junction channels (Cx43 and Cx40), or genes associated with cardiomyocyte contractility (Serca2a and PLN; Figure 4A). Adult cardiomyocytes expressing Pkm2 had elevated β-catenin downstream targets Cyclin D1 and c-Myc (Figure 4B) and cell cycle-promoting genes (*Cdc20*, *Cdk2* and *Ccnd2*, *Ccnb1*) but fewer cell cycle inhibitors (p21 and p27) compared with control (Figure 4B).

Having shown that Pkm2 overexpression increases cell cycle markers and β-catenin downstream signaling,

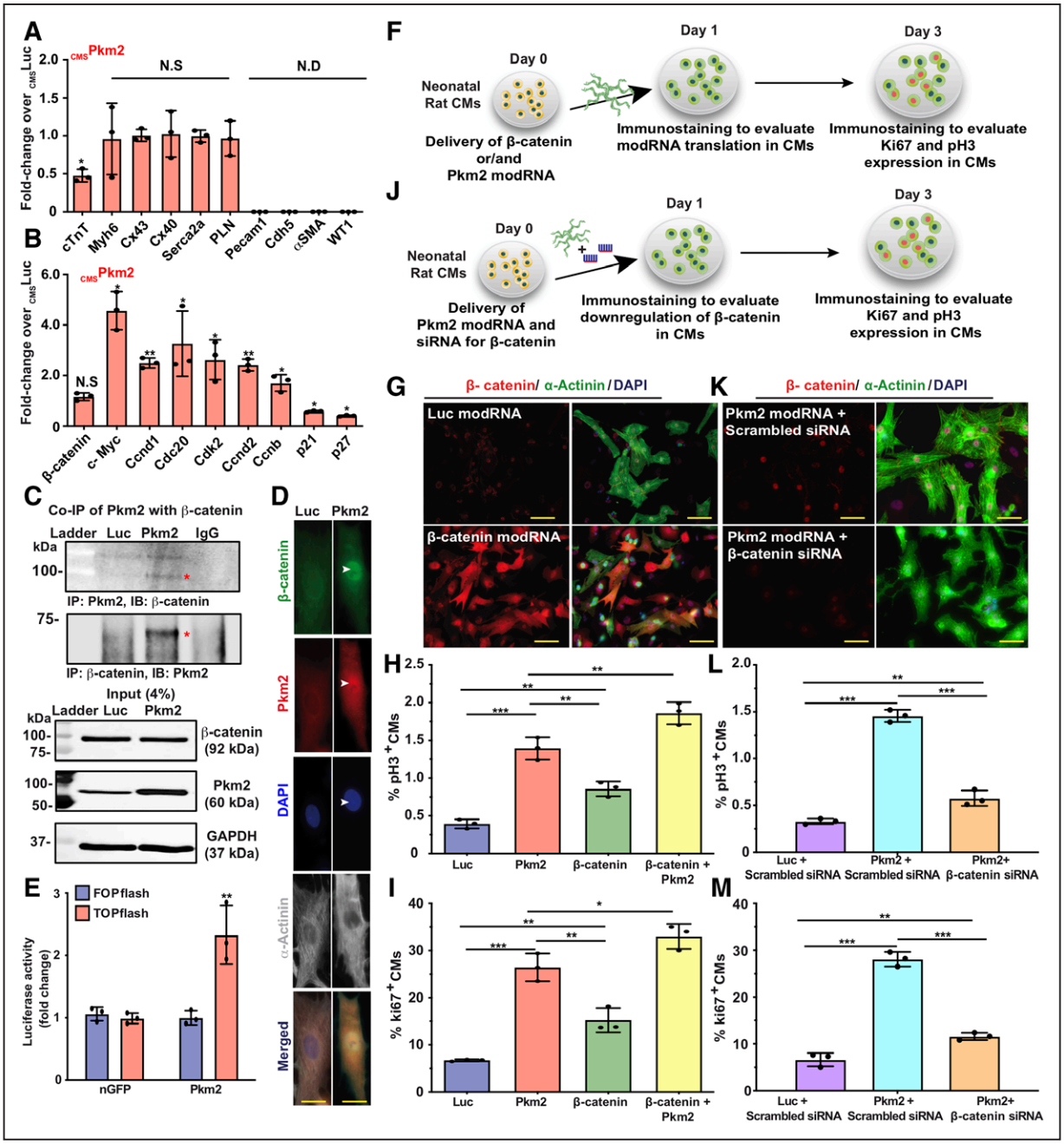

Figure 4. Pkm2 directly interacts with β-catenin, upregulates its downstream targets (Cyclin D1 and C-Myc), and increases expression of cell cycle–promoting genes and cell cycle markers in postnatal cardiomyocytes.

A and **B**, Two days after myocardial infarction (MI) and administration of cardiomyocyte-specific (cms) luciferase (Luc; cmsLuc) or cmsPkm2 modified RNAs (modRNAs) with cmsihCD25, adult cardiomyocytes were isolated using magnetic beads (please see method in Figure XIII in the Data Supplement). **A**, Quantitative real-time polymerase chain reaction analysis to validate purity of isolated cardiomyocytes, cardiomyocyte-specific markers, and functional cardiac genes (n=3). **B**, Gene expression comparisons of β-catenin downstream target genes and expression of cell-cycle-promoting genes or cell-cycle inhibitors after cmsLuc or cmsPkm2 modRNA delivery into adult cardiomyocytes (n=3). **C**, Coimmunoprecipitation (Co-IP) and input control to evaluate Pkm2's direct interaction with β-catenin in P3 rat neonatal cardiomyocytes after luciferase or Pkm2 modRNA transfection (n=2). **D**, Immunostaining of rat neonatal cardiomyocyte after luciferase or Pkm2 modRNA delivery shows co-localized β-catenin and Pkm2 in the cardiomyocyte nucleus. **E**, Stabilizing β-catenin induced its interaction with TCF/LEF transcription factors in the nucleus, which in turn induced the expression of target genes (eg, cyclin D1, c-Myc) that can be measured by TOPflash (Luciferase reporter with TCF binding DNA sequence). Fopflash has mutant TCF binding DNA sequence (Fopflash), used as control. Quantitative TOPflash or Fopflash after delivery of nGFP (control) or Pkm2 modRNA (n=3). **F**, Experimental plan for evaluating overexpression of β-catenin alone or with Pkm2 modRNA and studying its effect on the expression of cell cycle genes in P3 neonatal rat cardiomyocytes. **G**, Representative images of β-catenin expression 1 day after luciferase or β-catenin modRNA transfection in vitro (costained α-Actinin and DAPI). **H** and **I**, Quantification of cell cycle markers (Ki67, pH3) in neonatal rat cardiomyocytes 3 days after transfection of Luc, Pkm2, or β-catenin modRNA alone or combined Pkm2 and β-catenin modRNAs (n=3). **J**, Experimental timeline used to evaluate the role of β-catenin in cardiomyocytes after Pkm2 modRNA delivery. **K**, Representative images of β-catenin inhibition by siRNA in cardiomyocytes after Pkm2 modRNA delivery. **L** and **M**, Quantification of cell cycle markers (Ki67, pH3) in neonatal rat cardiomyocytes 3 days after transfection with luciferase or Pkm2 modRNA with scrambled siRNA or Pkm2 modRNA with siRNA for β-catenin (n=3). One-way ANOVA, Tukey's Multiple Comparison Test for **A** and **B**, **H** and **I**, **L** and **M**. Unpaired 2-tailed *t* test for **E**. ***P<0.001, **P<0.01, *P<0.05, N.S., not significant, N.D., no data. Scale bar, 10 μm (**D**) and 25 μm (**G**) and (**K**). CM indicates cardiomyocyte; DAPI, 4′,6-diamidino-2-phenylindole; GAPDH, Glyceraldehyde 3-phosphate dehydrogenase; LAD, left anterior descending coronary artery; and Pkm2, pyruvate kinase muscle isoenzyme 2.

and because Pkm2 has been shown to interact directly with β-catenin in prostate cancer cells, we performed a coimmunoprecipitation assay (Figure 4C), which revealed that Pkm2 directly interacts with β-catenin in cardiomyocytes. We also showed β-catenin and Pkm2 colocalization in the cardiomyocyte nuclei (Figure 4D). In addition, we performed a TOPFlash luciferase assay to track β-catenin/TCF activity and demonstrated that Pkm2 modRNA increased β-catenin activation in neonatal rat cardiomyocytes in vitro (Figure 4E).

To better understand the β-catenin pathway's role in the Pkm2-induced cardiomyocyte cell cycle, we made β-catenin modRNA and transfected it, alone or with Pkm2, into neonatal rat cardiomyocytes in vitro. Our results reveal significantly elevated cell cycle markers in cardiomyocytes 3 days after delivery of each gene alone, in comparison with luciferase modRNA. However, Pkm2 modRNA generated significantly ($P \leq 0.001$) higher cell marker expression in cardiomyocytes than β-catenin (Figure 4F through 4I), thereby suggesting that the β-catenin pathway is not the only pathway Pkm2 uses to promote cardiomyocyte cell division. Also, we show that adding Pkm2 modRNA to β-catenin increased cell cycle marker expression in cardiomyocytes, indicating a synergistic effect between the 2 genes (Figure 4H and 4I). To further decipher the role of β-catenin in the Pkm2-induced cardiomyocyte cell cycle, we transfected rat neonatal cardiomyocytes with Pkm2 modRNA concomitantly with β-catenin knockdown (Figure 4J through 4M). Our results show the β-catenin pathway is important for inducing cell cycle marker expression in cardiomyocytes (Figure 4L and 4M). Yet even without β-catenin, Pkm2 raises cell cycle marker expression in cardiomyocytes, in comparison with control, again suggesting a parallel pathway that increases cardiomyocyte cell division and is independent from the β-catenin pathway (Figure 4L and 4M).

As Pkm2 plays a role in activating the anabolic pathway PPP by elevating G6pd, the rate-limiting enzyme of PPP, in a human lung cancer cell line,[42] we wanted to discover if Pkm2 overexpression in cardiomyocytes upregulates G6pd and thus alters anabolic metabolism. To investigate this, we transfected neonatal rat cardiomyocytes with luciferase or Pkm2 modRNA and collected the cells 2 days later (Figure XIIa in the Data Supplement). Western blot analysis showed increased G6pd after Pkm2 modRNA in comparison with control (Figure XIIb and XIIc in the Data Supplement). In addition, we used isotopic tracers to investigate metabolic flux by adding glucose to the media of neonatal rat cardiomyocytes 6 hours after Pkm2 or luciferase modRNA delivery and collecting samples to test glycolysis (after 10 minutes), TCA cycle (after 2 hours), or PPP (after 18 hours). Our results show elevated PPP and increased ribonucleotide synthesis. The latter has previously been shown to be important for inducing cell division, as ribonucleotides are the building blocks of nucleic acid needed for DNA synthesis (Figure XIId in the Data Supplement).[43]

Because the oxidative branch of the PPP is a major source of NADPH, we investigated whether Pkm2 overexpression to cardiomyocytes increases NADPH production. Indeed, our results show that Pkm2 modRNA raises NADPH production and reduces the $NADP^+$/NADPH ratio (Figure XIIe in the Data Supplement). As PPP activation is associated with reduced oxidative stress, reactive oxygen species (ROS) production, and oxidative DNA damage, we explored how intramyocardial delivery of $_{CMS}$Luc or $_{CMS}$Pkm2 modRNA influenced these processes and elevated G6pd after MI (Figure 5). Two days after MI, we transfected cardiomyocytes with either Pkm2 or luciferase and showed that Pkm2-transfected cardiomyocytes have higher G6pd expression (Figure 5A; isolation method described in Figure XI in the Data Supplement). High performance liquid chromatography measurements of oxidative stress (reduced/oxidized glutathione ratio, Figure 5B and 5C; superoxide and other ROS , Figure 5D and 5E; as well as immunostaining of 8-hydroxyguanosine, Figure 5F and 5G; or pATM, Figure 5H and 5I) all show less oxidative stress, less ROS production, and less oxidative DNA damage 2 days after MI and intramyocardial delivery of $_{CMS}$Pkm2, in comparison with control.

To evaluate G6pd and the role of anabolic pathway activation in the cardiomyocyte cell cycle, we made G6pd modRNA and transfected it, alone or with Pkm2, into neonatal rat cardiomyocytes in vitro. Our results reveal significantly more cell cycle markers in cardiomyocytes 3 days after delivery of each gene alone, in comparison with luciferase modRNA. However, Pkm2 modRNA generated significantly ($P \leq 0.01$) higher expression of cell cycle markers in cardiomyocytes than did G6pd (Figure 5J through 5M), thereby suggesting, similar to our β-catenin results (Figure 5H and 5I), that the G6pd pathway is not the only pathway that Pkm2 enhances to promote the cardiomyocyte cell cycle. Also, we show that adding Pkm2 modRNA to G6pd increased expression of the cell cycle marker Ki67 in cardiomyocytes, indicating a possible synergistic effect between the 2 genes (Figure 5M). To further decipher the role of G6pd in Pkm2-induced cell division in cardiomyocytes, we transfected rat neonatal cardiomyocytes with Pkm2 modRNA concomitantly with G6pd knockdown (Figure 5O through 5R). Our results indicate that G6pd and the anabolic pathway PPP are important for inducing cell cycle marker expression in cardiomyocytes (Figure 5Q and 5R). Yet even with less G6pd, Pkm2 increased cell cycle marker expression in cardiomyocytes as compared with control, suggesting again another pathway, parallel to, but independent from, β-catenin, that increases cardiomyocyte cell division (Figure 5Q and 5R). In sum, and as Figure 5 illustrates, we were able to show that Pkm2's anabolic enzymatic activity

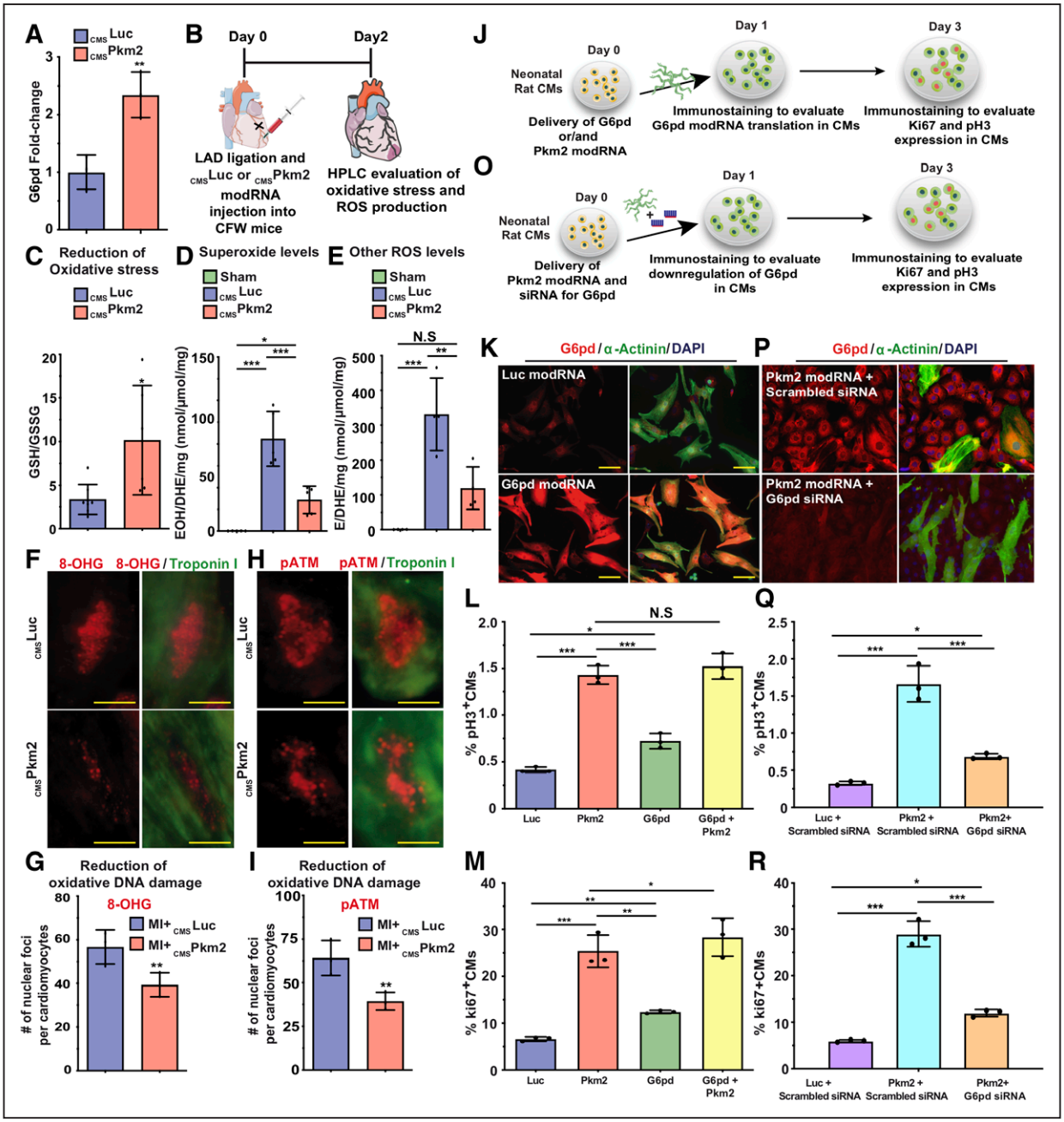

Figure 5. Pkm2 upregulates the anabolic enzyme G6pd, which reduces oxidative stress, reactive oxygen species production, and oxidative damage and leads to increased expression of cell cycle markers in postnatal cardiomyocytes.

A, Quantitative polymerase chain reaction comparisons of G6pd (glucose-6-phosphate dehydrogenase) expression 2 days after myocardial infarction (MI) and administration of cardiomyocyte-specific (cms) luciferase (Luc; cmsLuc) or cmsPkm2 modified RNAs (modRNAs) with cardiomyocyte-specific inactive human CD25 (cmsihCD25), when adult cardiomyocytes were isolated using magnetic beads (please see method in Figure XIII in the Data Supplement). **B**, Experimental timeline used to evaluate reduced oxidative stress or reactive oxygen species (ROS) production after MI and delivery of cmsLuc or cmsPkm2 modRNA. **C**, High performance liquid chromatography (HPLC) quantification of GSH/GSSG ratio (reduced/oxidized glutathione), n=6. **D** and **E**, HPLC quantification of superoxide probe dihydroethidium (DHE) in (**D**) 2-hydroxyethidium (EOH), n=5, or (**E**) ethidium (E), n=4, 2 days after MI and cmsLuc or cmsPkm2 modRNA injection or sham operation. **F**, Representative images of 8-OHG (8-hyrdroxyguanosine) foci frequency in cardiomyocytes 2 days after MI and transfection with either CMSLuc or CMSPkm2 modRNA (costained α-Actinin and DAPI). **G**, Quantitative analysis of **F**, n=3. **H**, Representative images of pATM (phosphorylation of ataxia telangiectasia mutated) foci frequency in cardiomyocytes 2 days after MI and transfection with CMSLuc or CMSPkm2 modRNA. **I**, Quantitative analysis of **H**, n=3. **J**, Experimental plan for evaluating overexpression of G6pd alone or with Pkm2 modRNA and studying its effect on the expression of cell cycle genes in P3 neonatal rat cardiomyocytes. **K**, Representative images of G6pd expression 1 day after luciferase or G6pd modRNAs transfection in vitro (costained α-Actinin and DAPI). **L** and **M**, Quantification of cell cycle markers (Ki67, pH3) in neonatal rat cardiomyocytes 3 days after transfection of Luc, Pkm2 or G6pd modRNA alone or combined Pkm2 and G6pd modRNAs, n=3. **O**, Experimental timeline used to evaluate the role of G6pd in cardiomyocytes after Pkm2 modRNA delivery. **P**, Representative images of G6pd inhibition by siRNA in cardiomyocytes after Pkm2 modRNA delivery. **Q** and **R**, Quantification of cell cycle markers (Ki67, pH3) in neonatal rat cardiomyocytes 3 days after transfection with luciferase or Pkm2 modRNA with scrambled siRNA or Pkm2 modRNA with siRNA for G6pd, n=3. One-way ANOVA, Tukey's multiple comparison test for **L**, **M**, **Q**, and **R**. Unpaired 2-tailed *t* test for **A**, **C** through **E**, **G**, and **I**. ***P<0.001, **P<0.01, *P<0.05, N.S, not significant. Scale bar, 5 µm (**D**) and 25 µm (**G** and **K**). CM indicates cardiomyocyte; DAPI, 4′,6-diamidino-2-phenylindole; LAD, left anterior descending coronary artery; and Pkm2, pyruvate kinase muscle isoenzyme 2.

in cardiomyocytes changes glucose flux and raises anabolic PPP. Upregulating the PPP reduces oxidative stress, ROS production, and oxidative DNA damage, which in turn increases cardiomyocyte cell division.

Our data suggest that Pkm2 has at least 2 independent mechanisms of action that may influence cardiomyocyte cell division. One is the enzymatic anabolic pathway (G6pd and PPP) and the other is the nonenzymatic β-catenin pathway. As both pathways are important for cardiomyocyte cell division and because Pkm2 is highly expressed during development but not in adulthood, we wanted to evaluate its role in embryonic cardiomyocyte cell division and cardiac development. We generated inducible cardiomyocyte-specific Pkm2 knockout mice ($_{CMS}$KO-Pkm2, Figure 6A). We crossed either Pkm2$^{fl/fl}$ or Pkm2$^{+/+}$ with Tnnt2$^{MerCreMer/+}$ mice to generate either $_{CMS}$KO-Pkm2 or $_{CMS}$WT mice, respectively. Both $_{CMS}$KO-Pkm2 and $_{CMS}$WT mice received tamoxifen injections at E9 and E10 to flox out Pkm2 during cardiac development in $_{CMS}$KO-Pkm2 mice (Figure 6B). Because most $_{CMS}$KO-Pkm2 mice (>95%) died immediately after birth, we collected and evaluated hearts at E18. The E18 $_{CMS}$KO-Pkm2 and $_{CMS}$WT mice were similar in size (Figure 6C and 6D). As expected, no Pkm2 expression was seen in cardiomyocytes from $_{CMS}$KO-Pkm2 hearts (Figure 6E). We also observed significantly smaller hearts with thinner ventricular walls compared with control $_{CMS}$WT hearts (Figure 6F and 6G). The heart weight/body weight ratio was ≈17% lower in $_{CMS}$KO-Pkm2 mice than in $_{CMS}$WT mice (Figure 6H). Wheat agglutinin staining showed that cardiomyocytes from $_{CMS}$KO-Pkm2 hearts were ≈36% larger (Figure 6I and 6J), were ≈25% fewer in number (Figure 6K and 6L) and showed ≈54% less expression of cell cycle markers (Figure 6M through 6O) in comparison with cardiomyocytes from $_{CMS}$WT hearts. Moreover, in vitro cardiomyocytes isolated from E18 $_{CMS}$KO-Pkm2 hearts showed ≈59% lower expression of cell cycle markers than cardiomyocytes isolated from E18 $_{CMS}$WT hearts (Figure 6P through 6R). Gene expression comparison between $_{CMS}$KO-Pkm2 hearts and $_{CMS}$WT hearts shows that lack of Pkm2 in cardiomyocytes during development results in significantly lower Pkm2 downstream targets β-catenin, G6pd, c-Myc, and Ccnd1 (Figure 6S). Yet, cell cycle inhibitor (P27), cardiac hypertrophy markers ANP and BNP, and Pkm1 mRNA and protein are all upregulated (Figure 6S and 6T). We also tested if Pkm2 modRNA can rescue and restore cell cycle marker expression in cardiomyocytes. Accordingly, we isolated cardiomyocytes from $_{CMS}$KO-Pkm2 and transfected them with luciferase or Pkm2 modRNA. Three days after transfection with Pkm2 modRNA, $_{CMS}$KO-Pkm2 cardiomyocytes showed significantly ($P \leq 0.001$) elevated cell cycle markers in comparison to luciferase modRNA (Figure XIII in the Data Supplement). Taken together, our data suggest that Pkm2 expression in cardiomyocytes is required for cardiomyocyte cell division and proper heart development.

As Pkm2 may promote cardiomyocyte survival after transplantation,[29] and based on the totality of our data, we propose that $_{CMS}$Pkm2 modRNA may prevent cardiac remodeling and improve heart function post MI. We used our double-blind, long-term mouse MI model and tested the effect of $_{CMS}$Pkm2 modRNA 28 days after MI (Figure 7A). Magnetic resonance imaging and echo studies revealed that $_{CMS}$Pkm2 significantly increased the ejection fraction percentage (Figure 7B and 7C; Movies II and III in the Data Supplement), and the percentage fractioning delta shortened between day 2 (baseline, Figure XIVa and XIVb in the Data Supplement) and day 28 after MI (Figure 7D). Although LV internal diameter end systole showed little change, the LV internal diameter end diastole was much larger in $_{CMS}$Pkm2 mice than in controls 28 days after MI (Figure XIVc and XIVd in the Data Supplement). Further, 28 days after MI, Pkm2 or $_{CMS}$Pkm2 expression significantly increased LV end diastolic or systolic posterior wall thickness (Figure XIVe and XIVf in the Data Supplement) and reduced cardiac scar formation (Figure 7E and 7F, for baseline sham please see Figure XIVg in the Data Supplement). $_{CMS}$Pkm2 intramyocardial delivery did not cause any abnormality (eg, angioma, edema) in cardiac tissue (Figure 7E and 7F). Note that $_{CMS}$Pkm2 produced smaller scars than Pkm2 modRNA, indicating that delivering Pkm2 exclusively to cardiomyocytes has superior beneficial effects. $_{CMS}$Pkm2 also produced notably higher heart weight to body weight ratios with smaller cardiomyocytes and increased capillary density compared with control (Figure 7G and 7H and Figure XIVh through XIVj in the Data Supplement). Further, $_{CMS}$Pkm2 significantly raised cardiomyocyte numbers in the heart without elevating the number of nuclei per cardiomyocyte and increased the mononuclear fraction compared with control (Figure 7J through 7M). Of note, mice treated with $_{CMS}$Pkm2 modRNAs immediately after MI had significantly better long-term survival than those treated with $_{CMS}$Luc control (Figure 7N). We next used our chronic MI mouse model to evaluate $_{CMS}$Pkm2 modRNA's ability to reverse cardiac remodeling. In this model, we delivered modRNA intramyocardially 15 days after MI and then tracked ongoing cardiac remodeling (Figure 7O). Our results show significantly improved cardiac function (Figure 7P), increased expression of the cardiomyocyte cell cycle marker pH3 (Figure 7Q), and higher heart weight to body weight ratios (Figure 7R), with no significant change in cardiomyocyte size (Figure 7S). Taken together, our data reveal that $_{CMS}$Pkm2 modRNA has clear therapeutic effects on cardiomyocytes: it induces the cardiomyocyte cell cycle during cardiac development and after chronic or acute MI, increases angiogenesis, extends cardiomyocyte survival, and reduces both cardiomyocyte apoptosis and

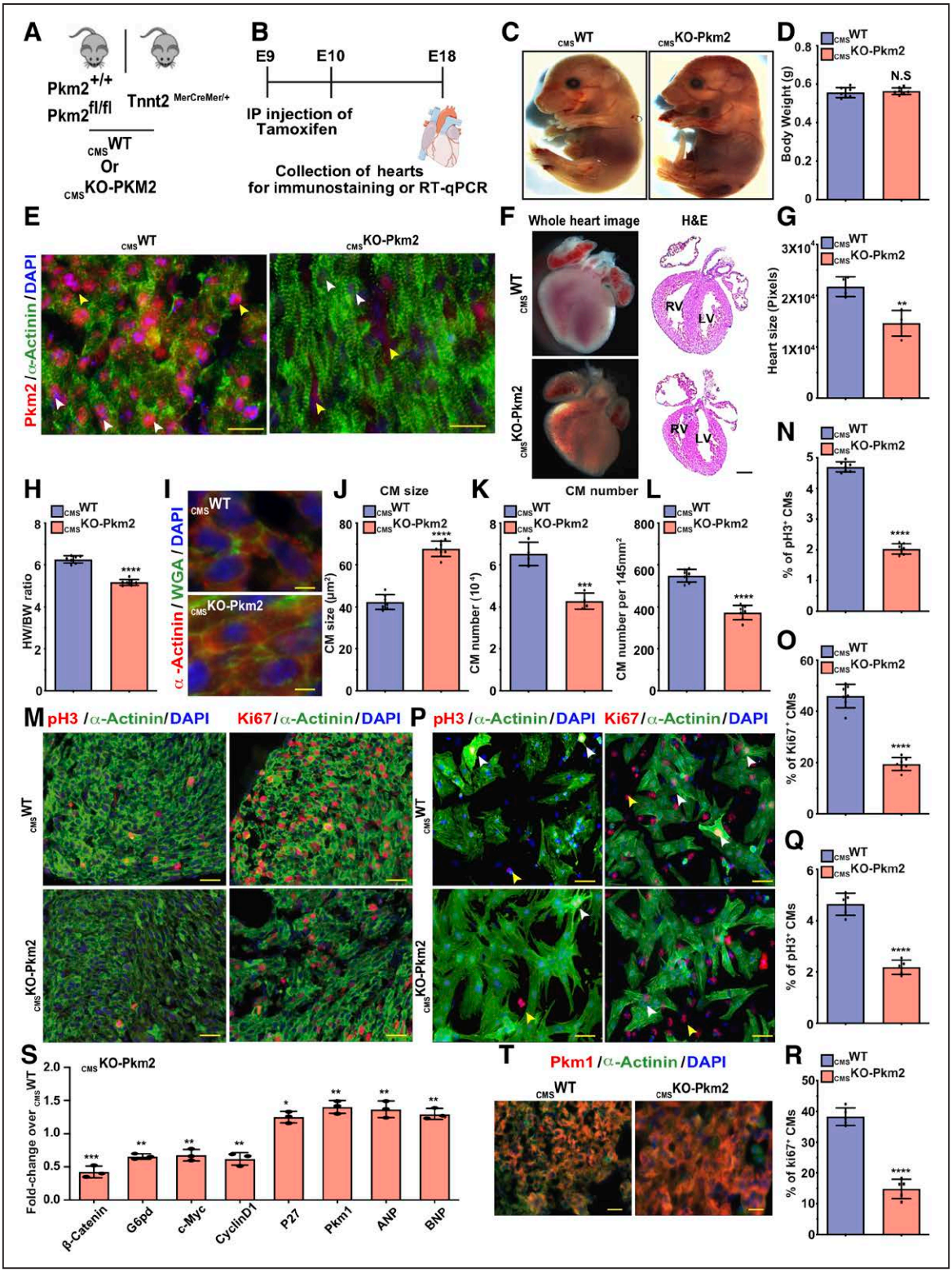

Figure 6. Loss of function study of Pkm2 expression in cardiomyocytes during heart development reduces heart size, increases cardiomyocyte size, lowers total cardiomyocyte number, and limits cardiomyocyte cell division capacity.

A, Experimental plan for generating inducible cardiomyocyte-specific wild type ($_{CMS}$WT; Pkm2+/+, B6129SF2/J) littermates expressing Cre exclusively in cardiomyocytes, or cardiomyocyte-specific Pkm2 knockout mice ($_{CMS}$KO-Pkm2). **B**, Experimental timeline for evaluating the effect of $_{CMS}$KO-Pkm2 on cardiomyocyte cell division and heart development. **C**, Representative images of E18 $_{CMS}$WT or $_{CMS}$KO-Pkm2 mice and (**D**) evaluation of body weight, n=7. **E**, Representative images of Pkm2 and α-Actinin immunostaining as well as whole heart hematoxylin and eosin staining F. Evaluation of heart size (G. n=4) and heart weight to body weight ratio (H. n=7) of E18 $_{CMS}$WT or $_{CMS}$KO-Pkm2. Representative images (**I**) of wheat germ agglutinin (WGA) and (**J**) quantification thereof, n=7. Quantification of cardiomyocyte numbers isolated from heart (**K**), n=4, or counted per section (**L**), n=7, in E18 $_{CMS}$WT or $_{CMS}$KO-Pkm2 mice. **M**, Representative images of pH3+ or Ki67+ cardiomyocytes in E18 $_{CMS}$WT or $_{CMS}$KO-Pkm2 hearts. Quantification of pH3+ (**N**), n=7, or ki67+ (**O**), n=7, cardiomyocytes in E18 $_{CMS}$WT or $_{CMS}$KO-Pkm2 hearts. (*Continued*)

Figure 6 Continued. **P**, Representative images of pH3- or Ki67-positive cardiomyocytes in isolated cardiomyocytes from E18 $_{CMS}$WT or $_{CMS}$KO-Pkm2 hearts. Quantification of pH3+ (**Q**), n=5, or ki67+ (**R**), n=5, cardiomyocytes isolated from E18 $_{CMS}$WT or $_{CMS}$KO-Pkm2 hearts. **S**, Relative gene expression measured by qRT-PCR comparing E18 $_{CMS}$WT or $_{CMS}$KO-Pkm2 hearts, n=3. **T**, Representative images of Pkm1 expression in E18 $_{CMS}$WT or $_{CMS}$KO-Pkm2 hearts. White arrowheads point to cardiomyocytes. Yellow arrowheads point to noncardiomyocytes. Unpaired 2-tailed *t* test for **D**, **G**, **H**, **J** through **L**, **N**, **O**, **Q**, **R**, and **S**. ****P<0.0001, ***P<0.001, **P<0.01, *P<0.05, N.S, not significant. Scale bar, 25 μm (**E** and **T**), 5 μm (**I**), 50 μm (**M** and **P**). CM indicates cardiomyocyte; DAPI, 4′,6-diamidino-2-phenylindole; LV, left ventricle; RV, right ventricle; and Pkm2, pyruvate kinase muscle isoenzyme 2.

oxidative stress to prevent or reverse cardiac remodeling after MI (Figure XV in the Data Supplement).

DISCUSSION

Reactivating cardiomyocyte proliferation is crucial to successful cardiac regeneration. Both newts and zebrafish have high levels of cardiac regeneration via activation of endogenous cardiomyocyte cell division.[44–47] Also, in fetal mice and pigs, induction of cardiomyocyte cell division leads to cardiac regeneration.[48–50] Studies in vitro and in vivo have shown that after injury, adult mammalian cardiomyocytes can divide, an ability that can be stimulated by upregulating proproliferative ge

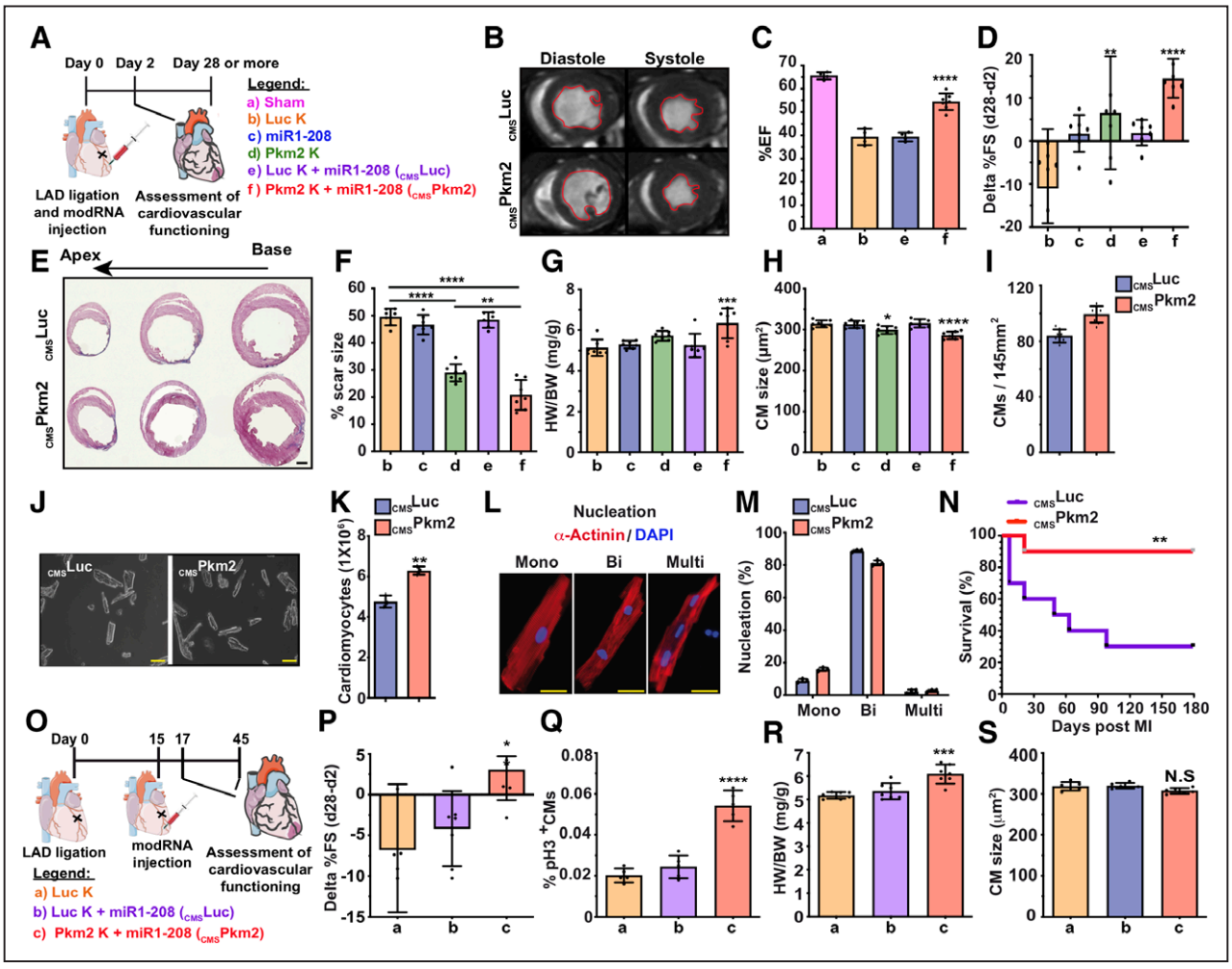

Figure 7. Gain of function study of Pkm2 expression in cardiomyocytes improves cardiac function and outcome after acute or chronic myocardial infarction. **A**, Experimental timeline to evaluate cardiac function and outcome in an acute myocardial infarction (MI) mouse model. **B**, Magnetic resonance imaging assessments of left ventricular systolic function 1 month after MI. Images depict left ventricular chamber (outlined in red) in diastole and systole. **C**, Percentage of ejection fraction for the experiments in (**B**); a, n=3; b, n=4; e, n=4; f, n=7. **D**, Echo evaluation of delta in percentage of fractioning shorting differences between day 2 (baseline) and day 28 after MI, n=7. **E**, Representative Masson trichrome staining to evaluate scar size 28 days after MI. **F** through **I**, Quantification of scar size (**F**), n=7; heart weight to body weight ratio (**G**), n=7; cardiomyocyte size (**H**), n=7; and cardiomyocyte numbers per section (**I**), n=8; measured 28 days after MI. Representative images (**J**) of cardiomyocyte numbers isolated from heart after treatments with cardiomyocyte-specific (CMS) luciferase (Luc; CMSLuc) or CMSPkm2 modified RNAs (modRNAs) 28 days after MI, and quantification (**K**) of the experiment in (**J**), n=3. **L**, Representative images of nuclei of isolated cardiomyocytes (mono, bi, or multi). **M**, Quantification of the experiment in (**L**), n=3. **N**, Long-term survival curve, after MI, for mice injected with cmsLuc or cmsPkm2 modRNAs, n=10. **O**, Experimental timeline to evaluate cardiac function and outcome in a chronic MI mouse model. **P**, Echo evaluation of delta in percentage of fractioning shorting differences between day 17 (baseline) and day 45 after MI, n=7. **Q** through **S**, Quantification of pH3+ cardiomyocytes in the heart (**Q**), n=5; heart weight (HW) to body weight (BW) ratio (**R**), n=7; or cardiomyocyte size (**S**), n=7; in the heart with different treatments 45 days after MI. White arrowheads point to cardiomyocytes. Yellow arrowheads point to noncardiomyocytes. One-way ANOVA, Bonferroni post hoc test for **C**, **D**, **F** through **I**, and **P** through **S**; unpaired 2-tailed *t* test for **J**, **K**, and **M**; Mantel-Cox log-rank test (**N**). ****P<0.0001, ***P<0.001, **P<0.01, *P<0.05, N.S, not significant. Scale bar, 1 mm (**E**), 50 μm (**K**), 10 μm (**L**). CM indicates cardiomyocyte; DAPI, 4′,6-diamidino-2-phenylindole; LAD, left anterior descending coronary artery; and Pkm2, pyruvate kinase muscle isoenzyme 2.

nes.[2,3,6,7,48,49,51–57] Other studies have shown that reactivating adult cardiomyocytes cell cycle reentry is possible via proteins[6,56,58] or viruses[59–61] and in transgenic mouse models of proproliferative genes.[2,5,7,51,53,54,62] Using proteins to induce the cell cycle is challenging because of their very short half-life, the difficulty of local administration, the lack of cardiomyocyte specificity, and their inability to deliver intranuclear genes, such as transcription factors. The cardiac-specific adeno-associated virus vector, though not immunogenic and relatively safe, has a long, sustained expression time that may lead to uncontrolled increases in cardiomyocyte size as well as cardiac hypertrophy and arrhythmia.[53] Although transgenic mice can be used as a model to study genes in cardiomyocytes, in transient or permanent conditions, this method is not clinically relevant for gene delivery.[54] The challenges posed by these current approaches emphasize the need for a safe, local, transient, efficient, and controlled method to deliver genes exclusively to cardiomyocytes.

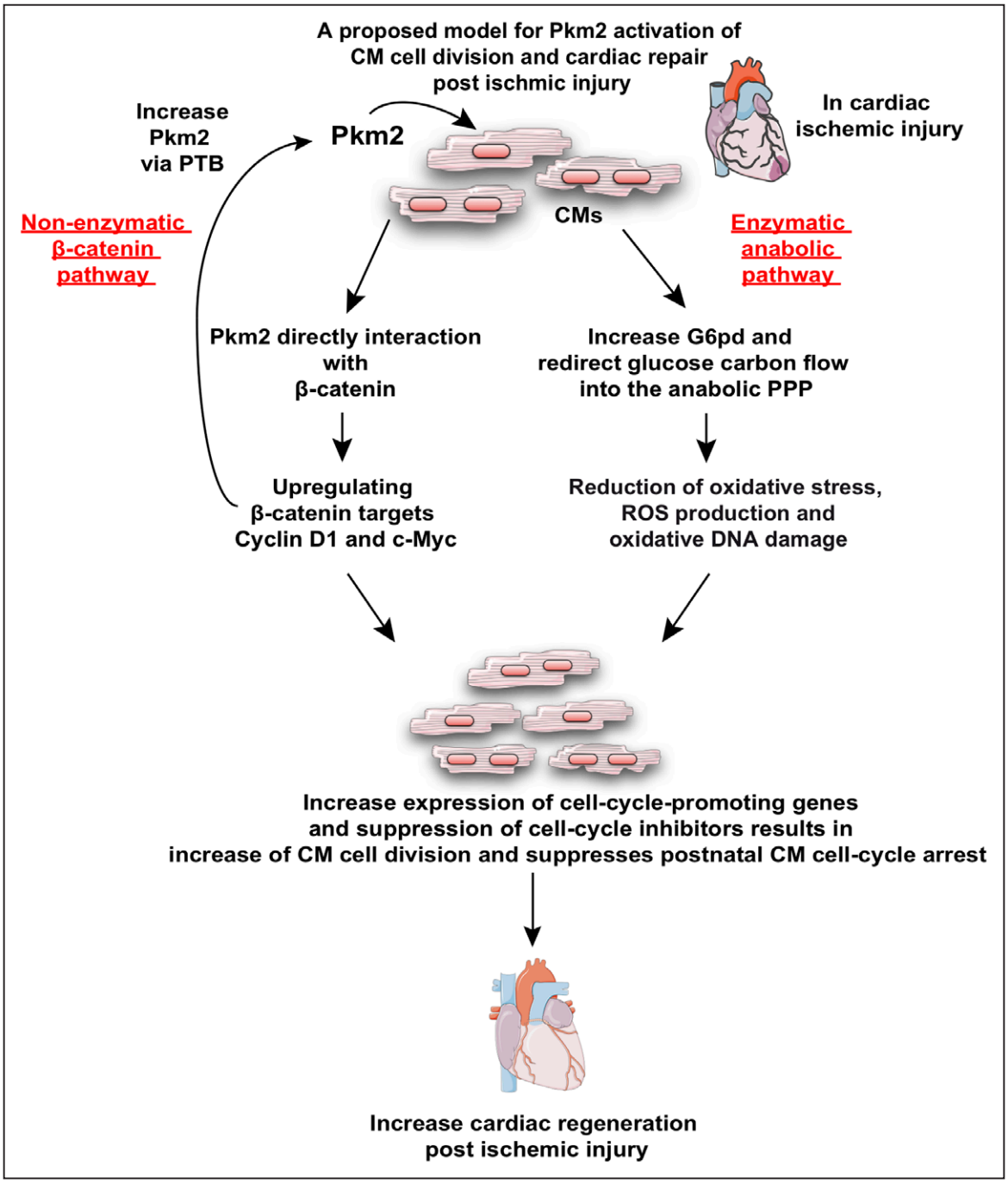

Figure 8. A proposed model for Pkm2 enzymatic (via G6pd) and nonenzymatic (via β-catenin) mechanisms of action that promote cardiomyocyte cell division, suppress postnatal cardiomyocyte cell-cycle arrest and increase cardiac regeneration post ischemic injury.
CM indicates cardiomyocyte; ROS, reactive oxygen species; and Pkm2, pyruvate kinase muscle isoenzyme 2.

In the current report, we demonstrate that Pkm2, which functions upstream of 2 nodal cardiomyocyte cell cycle regulatory pathways, is necessary and sufficient for inducing the cardiomyocyte cell cycle. On one hand, Pkm2 has a nonenzymatic function that directly interacts with β-catenin in cardiomyocyte nuclei, inducing β-catenin and upregulating its downstream targets Cyclin D1 and C-Myc (Figure 4). On the other hand, Pkm2 has an enzymatic function that elevates G6pd and redirects glucose carbon flow into the PPP anabolic pathway (Figure XII in the Data Supplement). PPP elevation results in decreased ROS production and oxidative DNA damage that suppresses postnatal cardiomyocyte cell cycle arrest (Figure 5). Identifying a single gene (*Pkm2*) that governs both pivotal pathways in cardiomyocytes may uncover a potential therapeutic approach for inducing cardiomyocyte cell division and regenerating the injured myocardium.

Overall, and as may be inferred from other cardiac studies,[28–30] our data suggest that endogenous Pkm2 upregulation in cardiomyocytes in response to ischemic injury is very limited in the adult heart and is insufficient to induce meaningful cardiomyocyte proliferation. Here we show that ectopic Pkm2 gene expression, specifically in cardiomyocytes, promotes both their cell division and cardiac regeneration. We show that previously identified cardiomyocyte proliferation pathways, including β-catenin, caERBB2, and Yap, may induce Pkm2 expression in neonatal cardiomyocytes (Figure XVI in the Data Supplement). Moreover, we show that Pkm2 is positively regulated by the β-catenin c-Myc, but not Cyclin D1. More specifically, we show that polypyrimidine tract binding protein-1, which is a target of c-Myc,[63] induces Pkm2 expression. These results suggest there is a positive feedback loop between Pkm2 and c-Myc that contributes to the cardiomyocyte cell cycle and cardiac regeneration. Moreover, our findings link the known cardiomyocyte cell cycle pathways (NRG1-ERBB signaling, Hippo-YAP signaling, hypoxia, and reduced ROS production) as NRG1-ERBB and Hippo-YAP signaling upregulate Pkm2 and thereby reduce ROS production in cardiomyocyte and increase their cell cycle (Figure 8; Figure XVI in the Data Supplement).

Our newly designed cardiomyocyte-specific delivery platform (Figure 2) overcomes cell-targeting challenges and opens new therapeutic opportunities for cardiac disease and regeneration. Cardiomyocyte-specific delivery using adeno-associated virus is limited because of its long-term gene expression (up to 11 months), which can have detrimental effects on cardiac regeneration.[54,64] Recently, Gabisonia et al showed that cardiac adeno-associated virus miR-199a in infarcted pigs stimulated cardiomyocyte cell division, but uncontrolled, long-term expression of this proproliferative gene eventually resulted in cardiac arrhythmia that led to sudden cardiac death.[64] By contrast, modRNA is a transient (expression lasts for 8 to 12 days), controlled, dose-dependent, gene delivery method. To date, however, modRNA delivery has only been used for upregulating in vivo paracrine factors such as VEGF-A,[33] IGF1,[65] and mutated human FSTL1[66] to propagate cardiac vascularization, protection, or regeneration, respectively. Because these factors act by binding to their cognate receptors on the cell surface, they are good candidates to study in a non–cell-specific system. Our newly designed system facilitates cardiomyocyte-specific modRNA gene delivery for both intracellular and intranuclear genes of interest. By developing cardiomyocyte-specific modRNA, we enable multiple platforms for the cardiovascular field. We were also able to introduce new lineage-tracing models using MADM mice (MADM-ML-11$^{GT/TG}$) and our cardiomyocyte-specific delivery of Cre (Figure 3), which is much faster and more cost-effective than a previously proposed MADM model,[40] and may be used by others to evaluate the roles of different genes of interest in inducing cardiomyocyte cell division in vivo. In this way, our current project is a proof of principle study showing that a short burst of cardiomyocyte proliferation either immediately or 2 weeks after MI may induce cardiac regeneration in a mouse model (Figure 7; Figure XIV in the Data Supplement). Future work should seek further development of cardiomyocyte-targeted modRNA delivery for clinical applications to induce cardiomyocyte cell cycle and cardiac regeneration.

ARTICLE INFORMATION

Received August 2, 2019; accepted February 28, 2020.

The Data Supplement is available with this article at https://www.ahajournals.org/doi/suppl/10.1161/circulationaha.119.043067.

Data sharing: All modified mRNA (modRNA) vectors containing any genes of interest in this paper will be made available to investigators. My institution and I will adhere to the National Institutes of Health Grants Policy on Sharing of Unique Research Resources including the "Sharing of Biomedical Research Resources: Principles and Guidelines for Recipients of National Institutes of Health (NIH) Grants and Contracts" issued in December 1999. https://grants.nih.gov/policy/sharing.htm. Specifically, material transfers would be made with no more restrictive terms than in the Simple Letter Agreement or the UBMTA and without reach through requirements. Should any intellectual property arise which requires a patent, we would ensure that the technology remains widely available to the research community in accordance with the NIH Principles and Guidelines document 66.

Correspondence

Lior Zangi, PhD, Ichan School of Medicine at Mount Sinai, 1 Gustave L. Levy Pl, New York, NY 10029. Email Lior.zangi@mssm.edu

Affiliations

Cardiovascular Research Center (A.M, N.S., A.A.K., I.M., T.M. K.B., M.T.K.S., E.C., Y.S., J.G.O., P.L, A.G.-S., C.K., M.M., L.Z.), Department of Genetics and Genomic Sciences (A.M, N.S., A.A.K., I.M., T.M. K.B., M.T.K.S., E.C., L.Z.), and Black Family Stem Cell Institute (A.M, N.S., A.A.K., I.M., T.M. K.B., M.T.K.S., E.C., L.Z.), Icahn School of Medicine at Mount Sinai, New York. King's College London British Heart Foundation Centre, School of Cardiovascular Medicine & Sciences, United Kingdom (C.X.C.X., M.M., A.M.S.). Proteomics and Metabolomics Core Facility, Weill Cornell Medicine, New York (G.Z.). Department of Pediatrics, Indiana University School of Medicine, Indianapolis (C.-L.C.). Phospholamban Foundation, Amsterdam, The Netherlands (R.J.H.).

Acknowledgments

The authors acknowledge Nishat Sultana, Yoav Hadas, Jason Kondrat, and Lu Zhang for their help with this article.

Sources of Funding

This work was funded by a cardiology start-up grant awarded to the Zangi laboratory and by NIH grant R01 HL142768-01. Dr Shah is supported by the British Heart Foundation.

Disclosures

Drs Zangi and Magadum are inventors of a Utility Patent Application (Cell-specific expression of modRNA, WO2018053414A1), which covers the results in this article. The other authors report no conflicts.

Supplemental Materials

Table of Contents
Expanded Methods and Materials
Data Supplement Figures I–XVI
Data Supplement Tables I–III
Data Supplement Movies I–III
Author Contributions
References 67–75

REFERENCES

1. Porrello ER, Mahmoud AI, Simpson E, Hill JA, Richardson JA, Olson EN, Sadek HA. Transient regenerative potential of the neonatal mouse heart. *Science.* 2011;331:1078–1080. doi: 10.1126/science.1200708
2. Heallen T, Zhang M, Wang J, Bonilla-Claudio M, Klysik E, Johnson RL, Martin JF. Hippo pathway inhibits Wnt signaling to restrain cardiomyocyte proliferation and heart size. *Science.* 2011;332:458–461. doi: 10.1126/science.1199010
3. Lin Z, von Gise A, Zhou P, Gu F, Ma Q, Jiang J, Yau AL, Buck JN, Gouin KA, van Gorp PR, et al. Cardiac-specific YAP activation improves cardiac function and survival in an experimental murine MI model. *Circ Res.* 2014;115:354–363. doi: 10.1161/CIRCRESAHA.115.303632
4. Morikawa Y, Heallen T, Leach J, Xiao Y, Martin JF. Dystrophin-glycoprotein complex sequesters Yap to inhibit cardiomyocyte proliferation. *Nature.* 2017;547:227–231. doi: 10.1038/nature22979
5. Xin M, Kim Y, Sutherland LB, Murakami M, Qi X, McAnally J, Porrello ER, Mahmoud AI, Tan W, Shelton JM, et al. Hippo pathway effector Yap promotes cardiac regeneration. *Proc Natl Acad Sci U S A.* 2013;110:13839–13844. doi: 10.1073/pnas.1313192110
6. Bersell K, Arab S, Haring B, Kühn B. Neuregulin1/ErbB4 signaling induces cardiomyocyte proliferation and repair of heart injury. *Cell.* 2009;138:257–270. doi: 10.1016/j.cell.2009.04.060
7. D'Uva G, Aharonov A, Lauriola M, Kain D, Yahalom-Ronen Y, Carvalho S, Weisinger K, Bassat E, Rajchman D, Yifa O, et al. ERBB2 triggers mammalian heart regeneration by promoting cardiomyocyte dedifferentiation and proliferation. *Nat Cell Biol.* 2015;17:627–638. doi: 10.1038/ncb3149
8. Nakada Y, Canseco DC, Thet S, Abdisalaam S, Asaithamby A, Santos CX, Shah AM, Zhang H, Faber JE, Kinter MT, et al. Hypoxia induces heart regeneration in adult mice. *Nature.* 2017;541:222–227. doi: 10.1038/nature20173
9. Puente BN, Kimura W, Muralidhar SA, Moon J, Amatruda JF, Phelps KL, Grinsfelder D, Rothermel BA, Chen R, Garcia JA, et al. The oxygen-rich postnatal environment induces cardiomyocyte cell-cycle arrest through DNA damage response. *Cell.* 2014;157:565–579. doi: 10.1016/j.cell.2014.03.032
10. Kimura W, Xiao F, Canseco DC, Muralidhar S, Thet S, Zhang HM, Abderrahman Y, Chen R, Garcia JA, Shelton JM, et al. Hypoxia fate mapping identifies cycling cardiomyocytes in the adult heart. *Nature.* 2015;523:226–230. doi: 10.1038/nature14582
11. Wong N, De Melo J, Tang D. PKM2, a central point of regulation in cancer metabolism. *Int J Cell Biol.* 2013;2013:242513. doi: 10.1155/2013/242513
12. Wu S, Le H. Dual roles of PKM2 in cancer metabolism. *Acta Biochim Biophys Sin (Shanghai).* 2013;45:27–35. doi: 10.1093/abbs/gms106
13. Yang W, Xia Y, Ji H, Zheng Y, Liang J, Huang W, Gao X, Aldape K, Lu Z. Nuclear PKM2 regulates β-catenin transactivation upon EGFR activation. *Nature.* 2011;480:118–122. doi: 10.1038/nature10598
14. Zhang J, Feng G, Bao G, Xu G, Sun Y, Li W, Wang L, Chen J, Jin H, Cui Z. Nuclear translocation of PKM2 modulates astrocyte proliferation via p27 and -catenin pathway after spinal cord injury. *Cell Cycle.* 2015;14:2609–2618. doi: 10.1080/15384101.2015.1064203
15. Kumar B, Bamezai RN. Moderate DNA damage promotes metabolic flux into PPP via PKM2 Y-105 phosphorylation: a feature that favours cancer cells. *Mol Biol Rep.* 2015;42:1317–1321. doi: 10.1007/s11033-015-3876-8
16. Noguchi T, Inoue H, Tanaka T. The M1- and M2-type isoenzymes of rat pyruvate kinase are produced from the same gene by alternative RNA splicing. *J Biol Chem.* 1986;261:13807–13812.
17. Dong G, Mao Q, Xia W, Xu Y, Wang J, Xu L, Jiang F. PKM2 and cancer: the function of PKM2 beyond glycolysis. *Oncol Lett.* 2016;11:1980–1986. doi: 10.3892/ol.2016.4168
18. Riganti C, Gazzano E, Polimeni M, Aldieri E, Ghigo D. The pentose phosphate pathway: an antioxidant defense and a crossroad in tumor cell fate. *Free Radic Biol Med.* 2012;53:421–436. doi: 10.1016/j.freeradbiomed.2012.05.006
19. Israelsen WJ, Dayton TL, Davidson SM, Fiske BP, Hosios AM, Bellinger G, Li J, Yu Y, Sasaki M, Horner JW, et al. PKM2 isoform-specific deletion reveals a differential requirement for pyruvate kinase in tumor cells. *Cell.* 2013;155:397–409. doi: 10.1016/j.cell.2013.09.025
20. Israelsen WJ, Vander Heiden MG. Pyruvate kinase: function, regulation and role in cancer. *Semin Cell Dev Biol.* 2015;43:43–51. doi: 10.1016/j.semcdb.2015.08.004
21. Chaneton B, Gottlieb E. Rocking cell metabolism: revised functions of the key glycolytic regulator PKM2 in cancer. *Trends Biochem Sci.* 2012;37:309–316. doi: 10.1016/j.tibs.2012.04.003
22. Muñoz ME, Ponce E. Pyruvate kinase: current status of regulatory and functional properties. *Comp Biochem Physiol B Biochem Mol Biol.* 2003;135:197–218. doi: 10.1016/s1096-4959(03)00081-2
23. Zheng X, Boyer L, Jin M, Mertens J, Kim Y, Ma L, Ma L, Hamm M, Gage FH, Hunter T. Metabolic reprogramming during neuronal differentiation from aerobic glycolysis to neuronal oxidative phosphorylation. *eLife.* 2016;5:pii :e13374. doi: 10.7554/eLife.13374
24. Luo W, Semenza GL. Pyruvate kinase M2 regulates glucose metabolism by functioning as a coactivator for hypoxia-inducible factor 1 in cancer cells. *Oncotarget.* 2011;2:551–556. doi: 10.18632/oncotarget.299
25. Mazurek S. Pyruvate kinase type M2: a key regulator of the metabolic budget system in tumor cells. *Int J Biochem Cell Biol.* 2011;43:969–980. doi: 10.1016/j.biocel.2010.02.005
26. Vander Heiden MG, Cantley LC, Thompson CB. Understanding the Warburg effect: the metabolic requirements of cell proliferation. *Science.* 2009;324:1029–1033. doi: 10.1126/science.1160809
27. Dayton TL, Gocheva V, Miller KM, Israelsen WJ, Bhutkar A, Clish CB, Davidson SM, Luengo A, Bronson RT, Jacks T, et al. Germline loss of PKM2 promotes metabolic distress and hepatocellular carcinoma. *Genes Dev.* 2016;30:1020–1033. doi: 10.1101/gad.278549.116
28. Rees ML, Subramaniam J, Li Y, Hamilton DJ, Frazier OH, Taegtmeyer H. A PKM2 signature in the failing heart. *Biochem Biophys Res Commun.* 2015;459:430–436. doi: 10.1016/j.bbrc.2015.02.122
29. Shi J, Yang X, Yang D, Li Y, Liu Y. Pyruvate kinase isoenzyme M2 expression correlates with survival of cardiomyocytes after allogeneic rat heterotopic heart transplantation. *Pathol Res Pract.* 2015;211:12–19. doi: 10.1016/j.prp.2014.10.003
30. Williams AL, Khadka V, Tang M, Avelar A, Schunke KJ, Menor M, Shohet RV. HIF1 mediates a switch in pyruvate kinase isoforms after myocardial infarction. *Physiol Genomics.* 2018;50:479–494. doi: 10.1152/physiolgenomics.00130.2017
31. Kondrat J, Sultana N, Zangi L. Synthesis of modified mRNA for myocardial delivery. *Methods Mol Biol.* 2017;1521:127–138. doi: 10.1007/978-1-4939-6588-5_8
32. Sultana N, Magadum A, Hadas Y, Kondrat J, Singh N, Youssef E, Calderon D, Chepurko E, Dubois N, Hajjar RJ, et al. Optimizing cardiac delivery of modified mRNA. *Mol Ther.* 2017;25:1306–1315. doi: 10.1016/j.ymthe.2017.03.016
33. Zangi L, Lui KO, von Gise A, Ma Q, Ebina W, Ptaszek LM, Später D, Xu H, Tabebordbar M, Gorbatov R, et al. Modified mRNA directs the fate of heart progenitor cells and induces vascular regeneration after myocardial infarction. *Nat Biotechnol.* 2013;31:898–907. doi: 10.1038/nbt.2682
34. Zangi L, Oliveira MS, Ye LY, Ma Q, Sultana N, Hadas Y, Chepurko E, Später D, Zhou B, Chew WL, et al. Insulin-like growth factor 1 receptor-dependent pathway drives epicardial adipose tissue formation after myocardial injury. *Circulation.* 2017;135:59–72. doi: 10.1161/CIRCULATIONAHA.116.022064

35. Ieda M, Tsuchihashi T, Ivey KN, Ross RS, Hong TT, Shaw RM, Srivastava D. Cardiac fibroblasts regulate myocardial proliferation through beta1 integrin signaling. *Dev Cell.* 2009;16:233–244. doi: 10.1016/j.devcel.2008.12.007
36. Hamma T, Ferré-D'Amaré AR. Structure of protein L7Ae bound to a K-turn derived from an archaeal box H/ACA sRNA at 1.8 A resolution. *Structure.* 2004;12:893–903. doi: 10.1016/j.str.2004.03.015
37. Wroblewska L, Kitada T, Endo K, Siciliano V, Stillo B, Saito H, Weiss R. Mammalian synthetic circuits with RNA binding proteins for RNA-only delivery. *Nat Biotechnol.* 2015;33:839–841. doi: 10.1038/nbt.3301
38. Zhao Y, Samal E, Srivastava D. Serum response factor regulates a muscle-specific microRNA that targets Hand2 during cardiogenesis. *Nature.* 2005;436:214–220. doi: 10.1038/nature03817
39. Williams AH, Liu N, van Rooij E, Olson EN. MicroRNA control of muscle development and disease. *Curr Opin Cell Biol.* 2009;21:461–469. doi: 10.1016/j.ceb.2009.01.029
40. Ali SR, Hippenmeyer S, Saadat LV, Luo L, Weissman IL, Ardehali R. Existing cardiomyocytes generate cardiomyocytes at a low rate after birth in mice. *Proc Natl Acad Sci U S A.* 2014;111:8850–8855. doi: 10.1073/pnas.1408233111
41. Mohamed TMA, Ang YS, Radzinsky E, Zhou P, Huang Y, Elfenbein A, Foley A, Magnitsky S, Srivastava D. Regulation of cell cycle to stimulate adult cardiomyocyte proliferation and cardiac regeneration. *Cell.* 2018;173:104–116.e12. doi: 10.1016/j.cell.2018.02.014
42. Salani B, Ravera S, Amaro A, Salis A, Passalacqua M, Millo E, Damonte G, Marini C, Pfeffer U, Sambuceti G, et al. IGF1 regulates PKM2 function through Akt phosphorylation. *Cell Cycle.* 2015;14:1559–1567. doi: 10.1080/15384101.2015.1026490
43. Fairbanks LD, Bofill M, Ruckemann K, Simmonds HA. Importance of ribonucleotide availability to proliferating T-lymphocytes from healthy humans. Disproportionate expansion of pyrimidine pools and contrasting effects of de novo synthesis inhibitors. *J Biol Chem.* 1995;270:29682–29689.
44. Bader D, Oberpriller JO. Repair and reorganization of minced cardiac muscle in the adult newt (Notophthalmus viridescens). *J Morphol.* 1978;155:349–357. doi: 10.1002/jmor.1051550307
45. Major RJ, Poss KD. Zebrafish heart regeneration as a model for cardiac tissue repair. *Drug Discov Today Dis Models.* 2007;4:219–225. doi: 10.1016/j.ddmod.2007.09.002
46. Poss KD, Wilson LG, Keating MT. Heart regeneration in zebrafish. *Science.* 2002;298:2188–2190. doi: 10.1126/science.1077857
47. Singh BN, Koyano-Nakagawa N, Garry JP, Weaver CV. Heart of newt: a recipe for regeneration. *J Cardiovasc Transl Res.* 2010;3:397–409. doi: 10.1007/s12265-010-9191-9
48. Leone M, Magadum A, Engel FB. Cardiomyocyte proliferation in cardiac development and regeneration: a guide to methodologies and interpretations. *Am J Physiol Heart Circ Physiol.* 2015;309:H1237–H1250. doi: 10.1152/ajpheart.00559.2015
49. Heo JS, Lee JC. β-Catenin mediates cyclic strain-stimulated cardiomyogenesis in mouse embryonic stem cells through ROS-dependent and integrin-mediated PI3K/Akt pathways. *J Cell Biochem.* 2011;112:1880–1889. doi: 10.1002/jcb.23108
50. Zhu W, Zhang E, Zhao M, Chong Z, Fan C, Tang Y, Hunter JD, Borovjagin AV, Walcott GP, Chen JY, et al. Regenerative potential of neonatal porcine hearts. *Circulation.* 2018;138:2809–2816. doi: 10.1161/CIRCULATIONAHA.118.034886
51. Beigi F, Schmeckpeper J, Pow-Anpongkul P, Payne JA, Zhang L, Zhang Z, Huang J, Mirotsou M, Dzau VJ. C3orf58, a novel paracrine protein, stimulates cardiomyocyte cell-cycle progression through the PI3K-AKT-CDK7 pathway. *Circ Res.* 2013;113:372–380. doi: 10.1161/CIRCRESAHA.113.301075
52. Engel FB, Schebesta M, Duong MT, Lu G, Ren S, Madwed JB, Jiang H, Wang Y, Keating MT. p38 MAP kinase inhibition enables proliferation of adult mammalian cardiomyocytes. *Genes Dev.* 2005;19:1175–1187. doi: 10.1101/gad.1306705
53. Lee HG, Chen Q, Wolfram JA, Richardson SL, Liner A, Siedlak SL, Zhu X, Ziats NP, Fujioka H, Felsher DW, et al. Cell cycle re-entry and mitochondrial defects in myc-mediated hypertrophic cardiomyopathy and heart failure. *PLoS One.* 2009;4:e7172. doi: 10.1371/journal.pone.0007172
54. Liao HS, Kang PM, Nagashima H, Yamasaki N, Usheva A, Ding B, Lorell BH, Izumo S. Cardiac-specific overexpression of cyclin-dependent kinase 2 increases smaller mononuclear cardiomyocytes. *Circ Res.* 2001;88:443–450. doi: 10.1161/01.res.88.4.443
55. Ozhan G, Weidinger G. Wnt/beta-catenin signaling in heart regeneration. *Cell Regen*. 2015;4:3. doi: 10.1186/s13619-015-0017-8
56. Kühn B, del Monte F, Hajjar RJ, Chang YS, Lebeche D, Arab S, Keating MT. Periostin induces proliferation of differentiated cardiomyocytes and promotes cardiac repair. *Nat Med.* 2007;13:962–969. doi: 10.1038/nm1619
57. Heallen T, Morikawa Y, Leach J, Tao G, Willerson JT, Johnson RL, Martin JF. Hippo signaling impedes adult heart regeneration. *Development.* 2013;140:4683–4690. doi: 10.1242/dev.102798
58. Wei K, Serpooshan V, Hurtado C, Diez-Cuñado M, Zhao M, Maruyama S, Zhu W, Fajardo G, Noseda M, Nakamura K, et al. Epicardial FSTL1 reconstitution regenerates the adult mammalian heart. *Nature.* 2015;525:479–485. doi: 10.1038/nature15372
59. Ebelt H, Zhang Y, Köhler K, Xu J, Gajawada P, Boettger T, Hollemann T, Müller-Werdan U, Werdan K, Braun T. Directed expression of dominant-negative p73 enables proliferation of cardiomyocytes in mice. *J Mol Cell Cardiol.* 2008;45:411–419. doi: 10.1016/j.yjmcc.2008.06.006
60. Engel FB. Cardiomyocyte proliferation: a platform for mammalian cardiac repair. *Cell Cycle.* 2005;4:1360–1363. doi: 10.4161/cc.4.10.2081
61. Eulalio A, Mano M, Dal Ferro M, Zentilin L, Sinagra G, Zacchigna S, Giacca M. Functional screening identifies miRNAs inducing cardiac regeneration. *Nature.* 2012;492:376–381. doi: 10.1038/nature11739
62. Mahmoud AI, Kocabas F, Muralidhar SA, Kimura W, Koura AS, Thet S, Porrello ER, Sadek HA. Meis1 regulates postnatal cardiomyocyte cell cycle arrest. *Nature.* 2013;497:249–253. doi: 10.1038/nature12054
63. Yang W, Zheng Y, Xia Y, Ji H, Chen X, Guo F, Lyssiotis CA, Aldape K, Cantley LC, Lu Z. ERK1/2-dependent phosphorylation and nuclear translocation of PKM2 promotes the Warburg effect. *Nat Cell Biol.* 2012;14:1295–1304. doi: 10.1038/ncb2629
64. Gabisonia K, Prosdocimo G, Aquaro GD, Carlucci L, Zentilin L, Secco I, Ali H, Braga L, Gorgodze N, Bernini F, et al. MicroRNA therapy stimulates uncontrolled cardiac repair after myocardial infarction in pigs. *Nature.* 2019;569:418–422. doi: 10.1038/s41586-019-1191-6
65. Huang CL, Leblond AL, Turner EC, Kumar AH, Martin K, Whelan D, O'Sullivan DM, Caplice NM. Synthetic chemically modified mRNA-based delivery of cytoprotective factor promotes early cardiomyocyte survival post-acute myocardial infarction. *Mol Pharm.* 2015;12:991–996. doi: 10.1021/mp5006239
66. Magadum A, Singh N, Kurian AA, Sharkar MTK, Chepurko E, Zangi L. Ablation of a single N-glycosylation site in human FSTL 1 induces cardiomyocyte proliferation and cardiac regeneration. *Mol Ther Nucleic Acids.* 2018;13:133–143. doi: 10.1016/j.omtn.2018.08.021
67. Tarnavski O, McMullen JR, Schinke M, Nie Q, Kong S, Izumo S. Mouse cardiac surgery: comprehensive techniques for the generation of mouse models of human diseases and their application for genomic studies. *Physiol Genomics.* 2004;16:349–360. doi: 10.1152/physiolgenomics.00041.2003
68. Engel FB, Hauck L, Cardoso MC, Leonhardt H, Dietz R, von Harsdorf R. A mammalian myocardial cell-free system to study cell cycle reentry in terminally differentiated cardiomyocytes. *Circ Res.* 1999;85:294–301. doi: 10.1161/01.res.85.3.294
69. Magadum A, Ding Y, He L, Kim T, Vasudevarao MD, Long Q, Yang K, Wickramasinghe N, Renikunta HV, Dubois N, et al. Live cell screening platform identifies PPARδ as a regulator of cardiomyocyte proliferation and cardiac repair. *Cell Res.* 2017;27:1002–1019. doi: 10.1038/cr.2017.84
70. Gorski PA, Kho C, Oh JG. Measuring Cardiomyocyte Contractility and Calcium Handling *In Vitro*. *Methods Mol Biol.* 2018;1816:93–104. doi: 10.1007/978-1-4939-8597-5_7
71. Saupe KW, Spindler M, Tian R, Ingwall JS. Impaired cardiac energetics in mice lacking muscle-specific isoenzymes of creatine kinase. *Circ Res.* 1998;82:898–907. doi: 10.1161/01.res.82.8.898
72. Buescher JM, Antoniewicz MR, Boros LG, Burgess SC, Brunengraber H, Clish CB, DeBerardinis RJ, Feron O, Frezza C, Ghesquiere B, et al. A roadmap for interpreting (13)C metabolite labeling patterns from cells. *Curr Opin Biotechnol.* 2015;34:189–201. doi: 10.1016/j.copbio.2015.02.003
73. Goncalves MD, Hwang SK, Pauli C, Murphy CJ, Cheng Z, Hopkins BD, Wu D, Loughran RM, Emerling BM, Zhang G, et al. Fenofibrate prevents skeletal muscle loss in mice with lung cancer. *Proc Natl Acad Sci U S A.* 2018;115:E743–E752. doi: 10.1073/pnas.1714703115
74. Fernandes DC, Wosniak J Jr, Pescatore LA, Bertoline MA, Liberman M, Laurindo FR, Santos CX. Analysis of DHE-derived oxidation products by HPLC in the assessment of superoxide production and NADPH oxidase activity in vascular systems. *Am J Physiol Cell Physiol.* 2007;292:C413–C422. doi: 10.1152/ajpcell.00188.2006
75. Ray PD, Huang BW, Tsuji Y. Reactive oxygen species (ROS) homeostasis and redox regulation in cellular signaling. *Cell Signal.* 2012;24:981–990. doi: 10.1016/j.cellsig.2012.01.008